Numerical Simulation of Low-Pressure Drop Static Mixers for Mixing Enhancement

Tariq, Syed Muhammad

Chemical Engineering Department, NED University of Engineering & Technology, Karachi, Sindh, PAKISTAN

Mushtaq, Asim**[+]

Polymer and Petrochemical Engineering Department, NED University of Engineering & Technology, Karachi, Sindh, PAKISTAN

Ullah, Ahmed; Qamar, Rizwan Ahmed; Ali, Zaeem Uddin; Hassan, Muhammad; Ahmed, Uzair; Alam, Syed Sarfaraz; Sadiq, Mariyam

Chemical Engineering Department, NED University of Engineering & Technology, Karachi, Sindh, PAKISTAN

ABSTRACT: *Static Mixers (SM), also generally known as inline mixers, form a newly developing industry trend. They have no moving parts, hence have lower energy consumption, lower installation cost, and very low maintenance cost, and are thus an attractive alternative to conventional agitators. Modifications were made to the design to reduce pressure drop and increase the mixing intensity across the mixer and increase the application of inline mixers in the industries. Three hybrid geometries (different combinations of Kenics and LPD) of static mixers were constructed and simulated using Computational Fluid Dynamics (CFD) tools. Kenics is an excellent radial mixing device, and Low-Pressure Drop (LPD) is an excellent axial mixing device. The key design parameter to modify LPD was the slope angle of elliptical plates which affects the mixer performance. Different slope angles from 90° to 120° were simulated. Kenics was modified for different aspect ratios, and the edge of Kenics was curved. Pressure drop, thermal, and Discrete Phase Model (DPM) analysis were performed on these three different classifications of hybrid geometries. The most promising geometry to emerge based on the low-pressure drop and good mixing efficiency was the curved edge Kenics. Keen-sighted these results, further analysis was performed on curved edge Kenics after the modification of the blend radius. It was concluded that for a lower Reynold number, the curved edge with a higher blend radius dominates all other mixers. Result validation was done by comparing the trends and sensitivity of process variables with the established results and standards.*

KEYWORDS: *Dynamic analysis; Static mixer; Computational fluid dynamics; Low-pressure drop; Curved edge kenics.*

INTRODUCTION

In the chemical industry, mixing is an essential procedure in various unit operations. A uniformly mixed system is created by physically bringing different components in contact. Depending on the application, mixing can be done on all states of matter, single and multi-phase systems, or miscible and immiscible fluids. Mixing plays a pivotal part in the product quality, capital cost, and outcome of the process. There are two ways to achieve mixing: with an agitator and without an agitator. The first method includes conventional mixers (like agitators, stirrers, impellers, and rotators), also called dynamic mixers because they have moving parts. Motors electrically power dynamic mixers, and the electrical energy is converted into rotary mechanical energy. The second method involves using static mixers, and as the name suggests, they do not have any moving parts [1, 2].

Fluid flow is an important parameter in the selection of mixing devices. Dynamic mixers are selected for the turbulent flow region. For highly viscous fluids and laminar flows, dynamic mixers require a high energy load; hence static mixers are preferred. Static Mixers (SM), also called motionless mixers are very easy to maintain as they do not have any moving parts. The fluid flow occurs in the Static Mixer (SM) due to the potential and kinetic energy of the fluid. Velocity gradients occur because of the flowing fluid's momentum. When the fluid flows through the static mixer, it splits, twists, shears, rotates and recombines the fluid stream. According to the process requirement, they are also applicable for continuous operations, Newtonian and non-Newtonian fluids. SM are preferred over dynamic mixers due to space constraints. Additional advantages include low residence time distribution, less erosion, scaling, near plug flow behavior, low operational cost, high radial mixing, and low equipment cost. A static mixer is a motionless mixing device enclosed in the pipe to manipulate the fluid streams by splitting, shearing, and recombining the streams as they flow towards the end of the pipe. Static mixers are not only used for mixing but also the reaction and heat transfer purposes. Radial mixing occurs inside an empty pipe (pipe without any resistance to the flow of fluid). Still, SMs significantly influences inline mixing and are fundamentally desirable for an inexpensive, fast, and continuous operation [3, 4].

In a static mixer, mixing energy exists in the form of pressure. Whether the material is fed to the mixer with an external pump or is gravity-fed, the pressure loss is the limiting factor in selecting the mixer and a major consequence of static mixing. Changes in the geometry of static mixers were made with time to suit various applications. Typical designs of static mixers include geometric grids at different angles, helical elements, baffles, and plates to increase turbulence and redirect flow stream, increasing the mixing efficiency. Changes in the geometry of SM also included the shapes of the mixing element. Generally, they had a round cross-section, but other shapes (like square and rectangular) were introduced for different applications. If an SM is sized and designed according to requirement, it helps achieve excellent single or multi-phase component mixing. The mixing performance of SM's is predicted based on pipe designing parameters, flow rate, and percentage of mixture components, viscosity, and density. In various cases, the number and types of mixing elements are selected to attain the best possible mixing without exceeding the acceptable pressure drop limit. Static mixers are a very economical alternative to the mixing application in the chemical industries. They help reduce cost by all means (be it equipment cost, operational, labor, or maintenance cost). The key parameter in selecting a static mixer is usually the pressure drop and mixing efficiency. To reduce the pressure drop, mixing efficiency is compromised and vice versa, which is the lagging point of static mixers. Hence in this report will explore a geometry that will help to minimize the pressure drop and increase the mixing intensity without compromising on any of the objectives [5, 6].

The main objective of this research is to modify the geometry of the static mixer while minimizing the pressure drop and maximizing the mixing efficiency. Numerous static mixer geometries are already being used at the industrial level (like Kenics, SMV, SMX, LLPD, and LPD SM's). The mixing intensity can be improved to increase mixing elements, but it readily increases the pressure drop. Thus, the objective of the research is to use hybrid geometry of mixing elements with an optimum crossing angle of the semi-elliptical plates in such a combination that will help achieve maximum mixing efficiency and minimum pressure drop. The performance of static mixers is analyzed through computational investigations, CFD simulations are run using ANSYS for hybrid geometry SMs. This study will focus on modifying the static mixer

with hybrid geometry. Much work has been done on single geometry SMs, but the field of hybrid geometries is yet to be extensively explored. This point can serve as both a positive and negative aspect of this research. The positive point is that it can be creative in geometry formation, and the negative aspect will occur during the result validation [7, 8].

Single geometry static mixers

They were mixing element design of type X. The type X bars are at 45° to the pipe axis. Laminar and turbulent flow both are applicable. To provide excellent mixing and dispersion. Very low product degradation because of minimum friction tension; hence is suitable for sensitive products for a compact static mixer design. The material was not choking in the pipeline because of cross mixing; only a few dead spots occurred. It gives a relatively high-pressure drop compared to other mixers [9]. X-crossed type mixing element design is modified. The pressure drop is 50% less as compared to the standard SMX. Applicable for wide viscosity range. It has an excellent mixing efficiency. It has a very short residence time, hence less product degradation. It has minimum shear stress, so suitable for sensitive products and excellent cross-mixing eliminates chances of material build-up inside the pipe. Compact design reduces capital cost for dispersing gases and liquids in high-viscous fluids. The task of adding a small amount of low-viscous additive into a high-viscous mainstream is performed very efficiently [10].

V-shaped mixing element design. Corrugated plates run at 30° or 45° along the axial direction through the pipe. Appropriate for gas mixing with a large contact surface. Suitable for short mixing lengths and large tube diameters (50 mm to infinity). Minimum space required for dispersion or mixing. Quick mass transfer through the uninterrupted renewal of the interface surface area. Fast & complete reaction, absorption, or extraction due to high mass transfer area. High mixing efficiency. They are applicable just in a turbulent flow [11].

Similar to Kenics with the only difference is that the individual mixing elements are tapered along their length and are slanted relative to the pipe axis. Twisted strips similar to the Kenics mixer, but they are conical ones with inclination, with no dead zones at the corners. No local superheating at the wall (important for heat-sensitive materials). Pressure and velocity variation along with the mixer. Low-pressure drop than Kenics. In comparison to

other static mixers, they have a 75% less pressure drop. Regardless of shape and size, they apply to the turbulent region. HEV mixer is typically applicable for low viscosity liquid-liquid blending processes and gas-gas mixing. HEV can easily be modified for non-circular cross sections and provides efficient blending in applications not suitable for traditional static mixers. Forgiven the degree of mixing, it gives the lowest pressure drop. It is easy to retrofit existing lines [12, 13].

ISG is a motionless mixer for continuous inline mixing. The mixer can quickly be installed in new and existing pipelines at low initial and operating costs. Since it has no moving parts, there is no wear, and as a result, no maintenance is required. ISG is easy to maintain as the mixer elements can be removed easily for separate cleaning. Four holes in each element provide a path for fluid flow, and the end of the element is designed to form a tetrahedral chamber. ISG mixing elements, the four holes are slanted such that material near the pipe wall at the inlet of the element appears near the center at the outlet. LPD SM contains semi-elliptical plates discriminately arranged in a tubular housing. They are applicable in both laminar and turbulent flow both. The fluid stream is continuously split and rotated at right angle clockwise and anti-clockwise directions as the product moves forward in the mixer. For liquids and gases with the low-pressure drop, LPD provides mathematically expected mixing results. Practically applicable for both viscous and non-viscous fluids [14, 15]. It contains semi-elliptical plates discriminately arranged in a tubular housing. Two panels are connected in the middle at 120° (one element). They are applicable in both laminar and turbulent flow both. Applicable for very low-pressure drop requirements. Comparing to LPD, the pressure drop of LLPD decreases by 0.46, and the L/D ratio increases from 1.5 to 1.75 [16, 17].

Modification in single geometry static mixer
SMX modification

The standard SMX mixer consists of multiple crossbars attached by an angle of 90°, and the elements are arranged in series axially through the housing length. By using standard SMX design resulting from the efficient mixing but more pressure drop. Hence the modification is still required to enhance the process efficiency of the mixer. Sudhanshu Soman investigated the effect of modifications in SMX design [18, 19]. The modifications in the SMX

design start with the perforations introduced on the blades of the mixing element. The first type of perforations was made in the mixing element. Initially, two holes as perforation of D/20 per blade were made and observed the pressure drop and the mixing performance. The basic purpose of this perforation is to enhance the mixer's efficiency by reducing its pressure drop and increasing mixing quality. So, more perforations were made, first by making four holes, then the maximum perforations of D/20 per blade were made, and the results were determined.

The results obtained by perforations show the reduced energy cost in pressure drop and better mixing quality. Hence, the idea was further examined, but the size of holes reduced D/30 and subsequently D/40. The fundamental idea behind increasing the number of perforations was that the size of each hole should be greater than the distance between two consecutive holes. Hence the maximum perforations were made of sizes D/30 and then D/40 per blade. The result was obtained by simulating these designs, and then these results were compared with the result obtained by standard SMX design. The next design was made by introducing the idea of serrations on each blade of the mixing element. The serration made on each blade provides more interfacial area resulting in better mixing quality, and the benefit of these serrated structures or design would significantly lower the pressure drop [18, 19].

The first idea was to introduce circular serrations. The fundamental idea was to introduce the maximum number of circular serrations per blade resulting in the maximum surface area, which reduces the energy lost; hence less pressure drop occurs. The serrations were made so that the diameter of each circular serrated region should be slightly lesser than the distance between two consecutive circles. Triangular notches along the blade length were the next modified serrated geometry of SMX. To increase the interfacial area, the serration used was the isosceles triangle having an angle of 45º, and sharp edges were filleted of 0.1 mm. And finally, the last modified SMX geometry was serrated using square notches having the length same as the radius of the circular serration since the pressure reduces by the sharp edges of the serrated body hence filleted by a radius of 0.1 mm [20, 21].

After designing these modifications, the simulation was analyzed, and all the modified geometries were then compared with standard SMX. The mixing quality was determined based on standard deviation, which is inversely

related to each other. The higher the standard deviation, the lower the mixing efficiency and vice versa. The simulated results were obtained and tabulated in Table 1 [22, 23].

Kenics modification

The optimal design of the Kenics mixer is chosen by comparing its geometries with different blade geometries (different twist angles and direction). The mixers are assessed based on their performance in terms of pressure drop. The results show that the standard design gives the best results. The standard design includes a 180º twist angle. Firstly, *Hobbs* and *Muzzio* studied limited angles because the velocity field had to be recomputed for each study. Hence angle 30º – 210º with the step of 30º were worked on and using stretching efficiency as a criterion. It was concluded that 120º is the most energy-efficient mixer. But now, with technology advancement, the quick analysis of results helped in a detailed study of angles, and 140º has yielded a distinct optimal twist angle. The criterion for this recent study was volume-flux weighed, sliced averaged, and discrete intensity of segregation [24].

LPD modification

Modifications in the LPD static mixer have been made in the angle between blades and the orientation of elements. The elements of the LPD static mixer consist of two semi-elliptical plates fitted with each other. The first semi-elliptical blade is the mirror image of the second one but fitted at an angle of 90º. Hence a series of these elements form the LPD static mixer [25]. The LPD static mixer is classified into two orientation designs, known as the right rotation– Right Rotation (RR) and right rotation– Left Rotation (RL) design. In the RR design, the neighboring element is the copy of the previous one but rotated at an angle of 90º in the tangential direction. In contrast, in the RL design, the second element is the mirrored image of the first one [1, 26]. The other modifications were made by changing the angle between the blades in the standard LPD mixer. The angle is 90º, so by varying the angles, the model's performance could be improved. Hence the design proposed to contain the angles 120º, 140º, and 160º, and the performance was determined. The result reveals that an increase in the angle between blades increases the mixing quality but at the cost of the drastic increase in length, which requires a larger area. Hence the LPD mixer

Table 1: Results of standard and modified SMX static mixers

Static Mixer	Mean Velocity (m/s)	Relative Standard Deviation (%)	Pressure Drop (Pa)
SMX	0.0006	54.8266	0.1185
Perforated SMX with 2 holes	0.00059	41.4651	0.1128
Perforated SMX with 4 holes	0.00059	28.9088	0.1101
Perforated SMX (D/20)	0.00058	21.5160	0.0905
Perforated SMX (D/30)	0.0006	16.2521	0.1117
Perforated SMX (D/40)	0.00058	50.3718	0.1197
SMX with Circular Serration	0.00056	23.9109	0.0787
SMX with Triangular Serration	0.00058	27.3613	0.0815
SMX with Square Serrations	0.00059	30.7914	0.1070

with a 120º blade angle was proposed as an optimum LPD static mixer and an LLPD static mixer [2].

Hybrid geometry static mixers

Hybrid geometry static mixer is an area less explored in the chemical industry. Some work has been done on the fusion of different static mixers. It can be found where Kenics and LPD were brought together, and different combinations of their mixing elements were investigated for their mixing performance and pressure drop by mathematically modeling it for two-phase flow (solid and fluid interaction). The results of this multi-mixer geometry were compared to the standard geometries for validation, and this experiment with multi-mixer geometry was deemed useful for future modifications. Two commonly used mixing devices in the industries for mixing purposes are LPD SM and Kenics SM. Static mixers show efficient mixing performance; comparing with Kenics, LPD requires low energy but entails a higher cost in reducing the pressure but has better mixing efficiency. The performance of Kenics mixers examined two different blade designs (based on their angle and twist direction) to conclude the optimum design [3].

This study concluded that the standard Kenics SM gives the desired performance in terms of pressure drop. Hence, six combinations were made using a total of four mixing elements of Kenics (T) and LPD (E), which were as follows: TTTT, EEEE, TETE, ETET, TEET, ETTE [4, 5]. The pressure drop by single and multi-phase flow was used to explore the mixing performance. The model was simulated by using mathematical modeling techniques, including FEM and DEM. Simulation-based on a couple

of DEM-FEM is used to examine the flow in the static mixer with six geometry combinations. The particle-particle and particle-to-mixer wall interactions are solved using Newton's law of motion. The simulation results conclude that for the TTTT combination, the pressure drop is the lowest, followed by TEET design but the mixing efficiency of TTTT is worse compared to other designs. Thus, conclude that the TEET geometry can contribute to the best mixing quality and an allowable pressure drop while significantly reducing the cost of the mixing process [6].

EXPERIMENTAL SECTION

The number of mixing elements can affect both the flow rate and mixing quality. When the number of elements increases, the resistance to the flow also increases, which is responsible for the decrease in flow rate passing through the mixer, but a greater number of elements means more splitting, spreading, and recombining the process stream in better mixing. *Gobel et al.* investigated the effect of mixing elements on mixing quality. They use the Discrete Element Method (DEM) for simulation, and the discrete element method code was validated using experimental results. Fig. 1 (a, b) shows the data is taken from their work and simplified for observing only the relationship between RSD and the number of mixing elements [4, 5, 6].

Their results reveal that increasing the number of elements from 1 to 4 significantly improves the mixing quality. Adding more than four mixing elements has no noticeable effect on the mixing quality or decreasing the relative standard deviation. After observing the results presented in the above paper, I also decided to choose four

Table 2: Blade geometry versus RSD value and blade design versus pressure drop

Geometry Combination	Relative Standard Deviation (%)	Pressure Drop (Pa)
EEEE	42.54	0.103793
ETTE	42.39	0.117287
ETET	40.59	0.111008
TTTT	37.6	0.013367
TETE	26.98	0.116478
TEET	20.32	0.083453

(a)

(b)
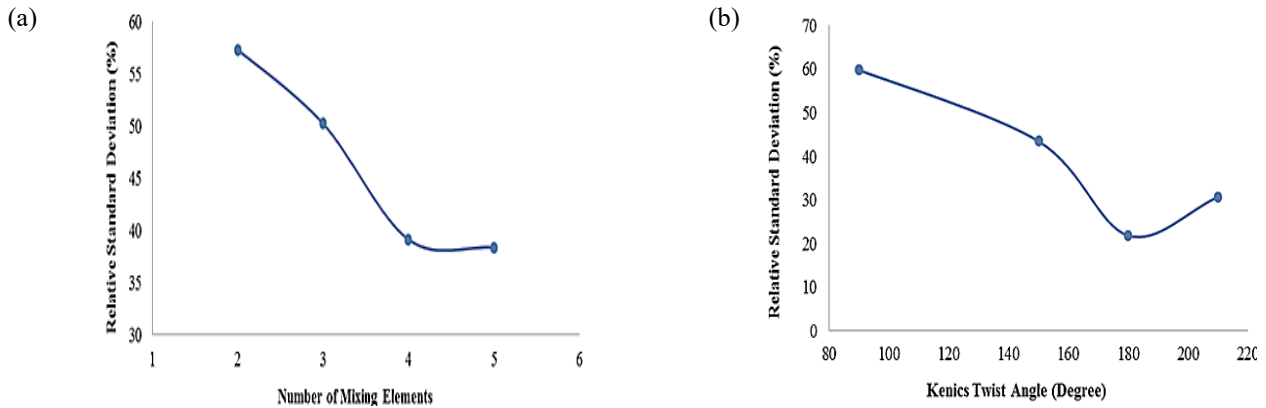
Fig. 1: (a) Mixing elements versus relative standard deviation (b) Kenics Twist Angle versus RSD.

mixing elements for the static mixer. A large variety of mixing elements are available in the market. Each one has its characteristics, and choosing the right one is the key to get the desired mixing. The energy required for mixing comes from the pressure drop across the mixer. Elements that have a higher pressure drop give high mixing and vice versa. Han *et al.* researched different types of mixing elements, including Kenics (RL 180º), the standard Sulzer SMX, the Ross Low-Pressure Drop (LPD RL 90º), and Low-Low Pressure Drop (LLPD) a fraction of their results are simplified 5.5, 3.8, 8.5 and 7.4 respectively [7, 8].

LPD is also very commonly use in the industries due to its simple design and low-pressure drop as compare to SMX and other compact variants of the static mixtures, so decided to make a hybrid mixer having LPD and Kenics. The Kenics helps to reduce the pressure drop and maintains it under the allowable range, while LPD makes the mixing more efficient. *F. Gobel et al.,* presented research in which twist angle of Kenics mixer was varied between 90º to 210º and slope angle of LPD mixer was varied between 30º to 60º. For describing the dynamics of the granular flow, the soft-sphere DEM simulation is used. The simulations were performed using the LIGGGHTS

open-source code. Results are simplified and shown in Fig. 1 (b) [9]. The result shows that; the Kenics twist angle highly influences the mixing quality, and the optimum twist angle for the Kenics mixer is 180º. Deviation from 180º result escaping of particles from the process of splitting and recombining which result in poor mixing quality. The optimum slope angle for LPD is 60º, and when the slope angle decreases, the pressure drop increases due to the lack of space available for the flow of particles inside the mixer. By observing the above results, LPD has a slope angle of 60º and Kenics with a twist angle of 180º.

The arrangement of mixing elements is also very important and different arrangement of both the Kenics and LPD gives different results. *Noraphon Bunklurab et al.* conducted a study in which six combinations are made, each one having four mixing elements, which include Kenics (T) with a twist angle of 180° and LPD (E) with the slope angle of 45°. The result of this study is simplified and mention in Table 2 [10]. The above results show that TEET has the least pressure drop, only second to TTTT, and having the lowest RSD value, which means higher mixing quality. So, by observing the above results, use the TEET combination for the hybrid mixer [11].

In the above article effect of different mixer arrangements, the element was observed. Still, there is no research or work done in manipulating the slope angle of the LPD using the TEET combination. As mentioned, the optimum slope angle for LPD is 60°. So, plan to conduct a study using different LPD slope angles in TEET combination and plan to change the aspect ratio for Kenics with a twist angle of 180°. Fig. 2 (a to m) shows the geometry number 1 to 9 of the mixing elements.

The experimental field, on the other hand, rested on the empirical models and contributed most to the engineering advancements. CFD, in the words of Anderson, constitutes a third approach along with pure experiments and pure theory [12, 13]. It bridges the gap between the two, makes it easy to comprehend and compare their results. Modern computing resources with an advanced numerical algorithm affect the understanding of fluids. Nevertheless, the CFD cannot replace the two tendencies. The advancement in theory and set of experimental data at the back is required to develop CFD [16].

Energy efficiency is based on the pressure drop per element normalized with an empty pipe of the same dimensions. This study reveals that the Kenics mixer has the lowest pressure drop because of its simple geometry design. In contrast, the standard SMX has the highest pressure drop due to its complex geometry or compactness, which requires a high-pressure drop to drive the fluid through it. *Galaktionov et al.*, find out the same results for the Kenics mixer [14, 15].

There are several numerical codes available to solve governing equations of fluid flow, albeit the framework of CFD remains the same. That framework is central in any analysis and defines the necessary steps involved in problem-solving through CFD analysis. This framework is broadly categorized into three stages; pre-processing, solver setup, and solution post-processing [16, 17]. It is the first stage of CFD analysis which involves building up the mathematical model by specifying the user inputs in terms of domain or geometry and physical phenomena involved like turbulence and specie transport [17]. After the mathematical model, the next step is meshing. The mathematical model is the translation of a physical phenomenon into mathematics [18, 19].

The optimization part is generally dependent on the aim of analysis and type of geometry. For simplified geometries with the intent of a general understanding of physics, the auto-generated mesh, which is coarse, sometimes could do the job. For complex geometries with sharp edges, curvature, and corners, though there are good meshing algorithms that do check for irregularities, it is better to go for optimization and to refine the mesh oneself [20]. Similarly, numerical methods introduce discretization errors. Both errors should be considered in any CFD analysis, and minimizing them as possible is necessary. The verification is also a part of pre-analysis and includes the reflection of solving the model right [21, 22]. The behavior of CFD results is analyzed to check whether they are consistent with hand calculations. Validation requires a comparison of experimental outcomes with CFD results. Good agreement of both is mandatory. Otherwise, reflection is required in modeling and numerical method to resolve any discrepancies [23, 24].

The mathematical model for static mixer

As this research utilizes the numerical simulation of hybrid static mixers to analyze the mixing performance and the pressure drop, the physical model being solved with its underlying principles and assumptions is the most fundamental factor to be accessed. The mathematical model always contains inherent errors that can be reduced by relaxing the assumptions and incorporating extensive coverage of physical aspects of the process. However, this more precise accuracy results in a more complex model, which is computationally expensive and requires long simulation runs. The key strategy to counter this challenge lies in "Multi-stage Modelling." This technique recommends starting with fewer physical aspects and more assumptions analyzing the results, and then building the model up towards more complexity until an optimized solution is achieved with realistic outcomes. Also, the appreciation of each amendment in the model can be fully understood [25, 26]. In the research of CFD, the mathematical model envisages; the domain or geometry and governing equation along with boundary conditions. Geometry is the base of any simulation and plays a very important role in engineering simulations. The ANSYS Design Modeler to make geometries of mixers [27, 28]. Design Modeler enables you to build up geometry from scratch, or you can also make CAD geometry modifications in it [1].
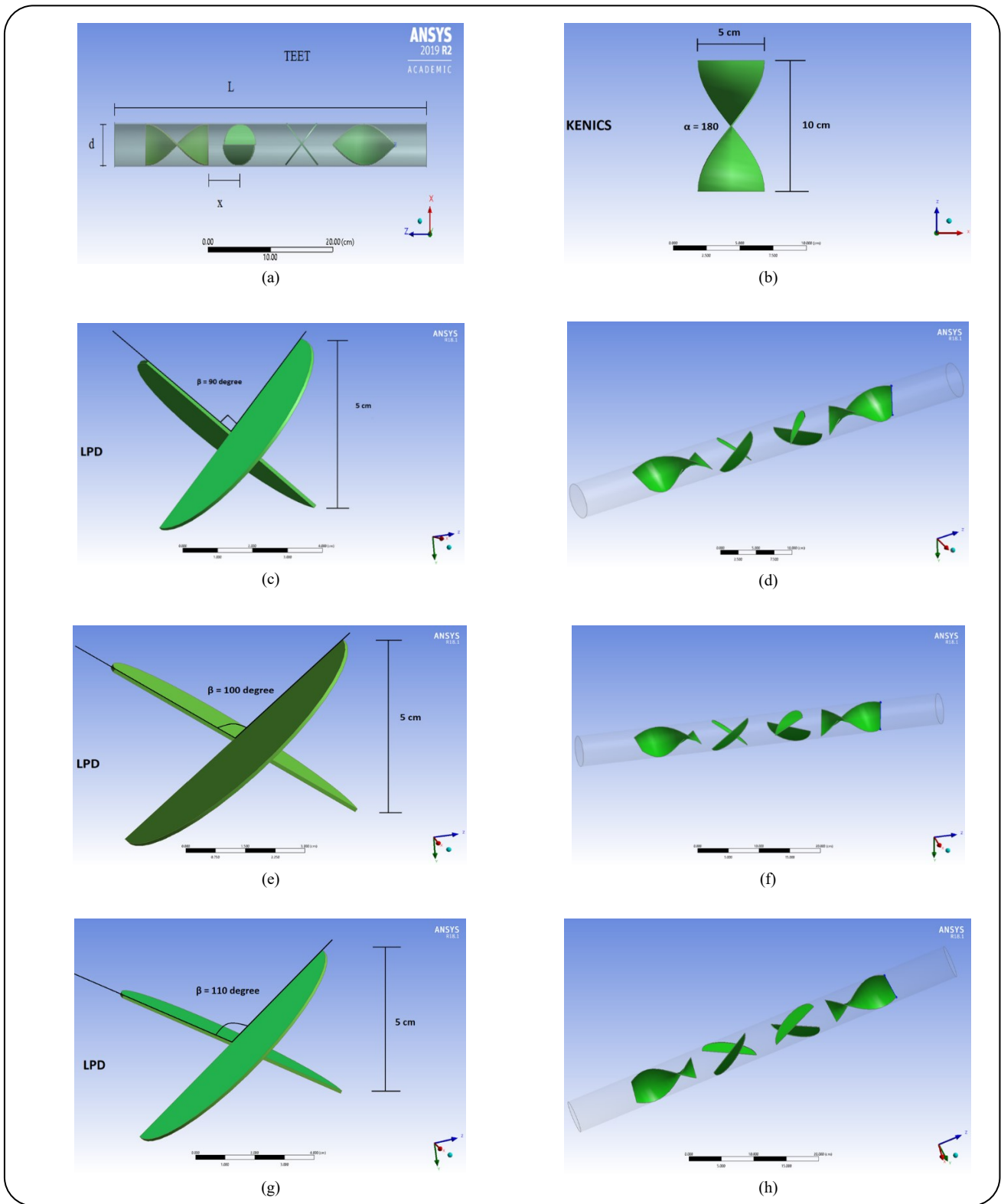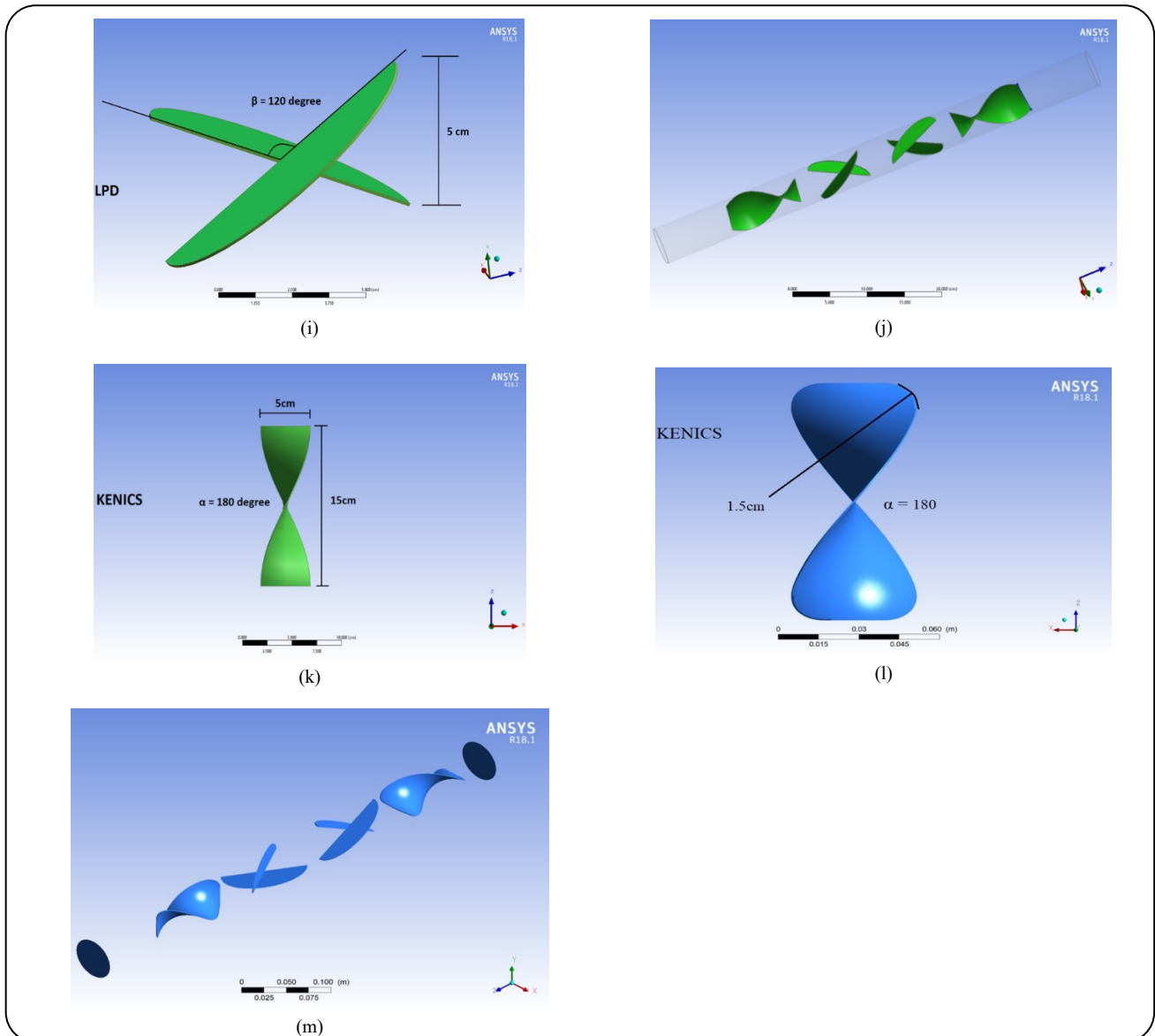
Fig. 2: Geometry number 1 to 9 (a) TEET static mixer (b) Twisted 1st mixing element (c) Elliptical element (d) TEET with 90° elliptical 2nd mixing element (e) 100° elliptical element (f) TEET with 100° elliptical element (g) 110° elliptical element (h) TEET with 110° elliptical element (i) 120° elliptical element (j) TEET with 120° elliptical element (k) Twisted Element with 3:1 aspect ratio (l) 1.5cm blend radius (m) curved edge geometry combination.

Fig. 2: Geometry number 1 to 9 (a) TEET static mixer (b) Twisted 1st mixing element (c) Elliptical element (d) TEET with 90° elliptical 2nd mixing element (e) 100° elliptical element (f) TEET with 100° elliptical element (g) 110° elliptical element (h) TEET with 110° elliptical element (i) 120° elliptical element (j) TEET with 120° elliptical element (k) Twisted Element with 3:1 aspect ratio (l) 1.5cm blend radius (m) curved edge geometry combination.

First, make a simple sketch of the ellipse, as shown in Fig. 3 (a), by using a sketch tool and dimension it to easily fit inside the 5cm pipe without leaving any gaps. Then transform it into an elliptical plate having a thickness of 0.1cm by using an extrude tool and make a mirror copy of the generated elliptical plate which is highlighted in Fig. 3 (b). The most important and the key step is to rotate both plates so that the crossing angle between them is β. LPD must fit perfectly inside the pipe without leaving any spaces or gaps, as shown in Fig. 3 (c) because

gaps and spaces promote escaping of mixing fluids and particles from the splitting and recombining process, which results in poor mixing quality. To make a Kenics in Design Modeler, make a simple rectangle having dimensions 5cm length, and 0.1cm width, which is the thickness of mixing element is shown in Fig. 3 (d). Then make a line of 10cm so that it is normal to the plane that generated the first sketch (rectangle). Now use the sweep tool, which extrudes the rectangular geometry along the reference line. A line created normal to the first sketch. After providing
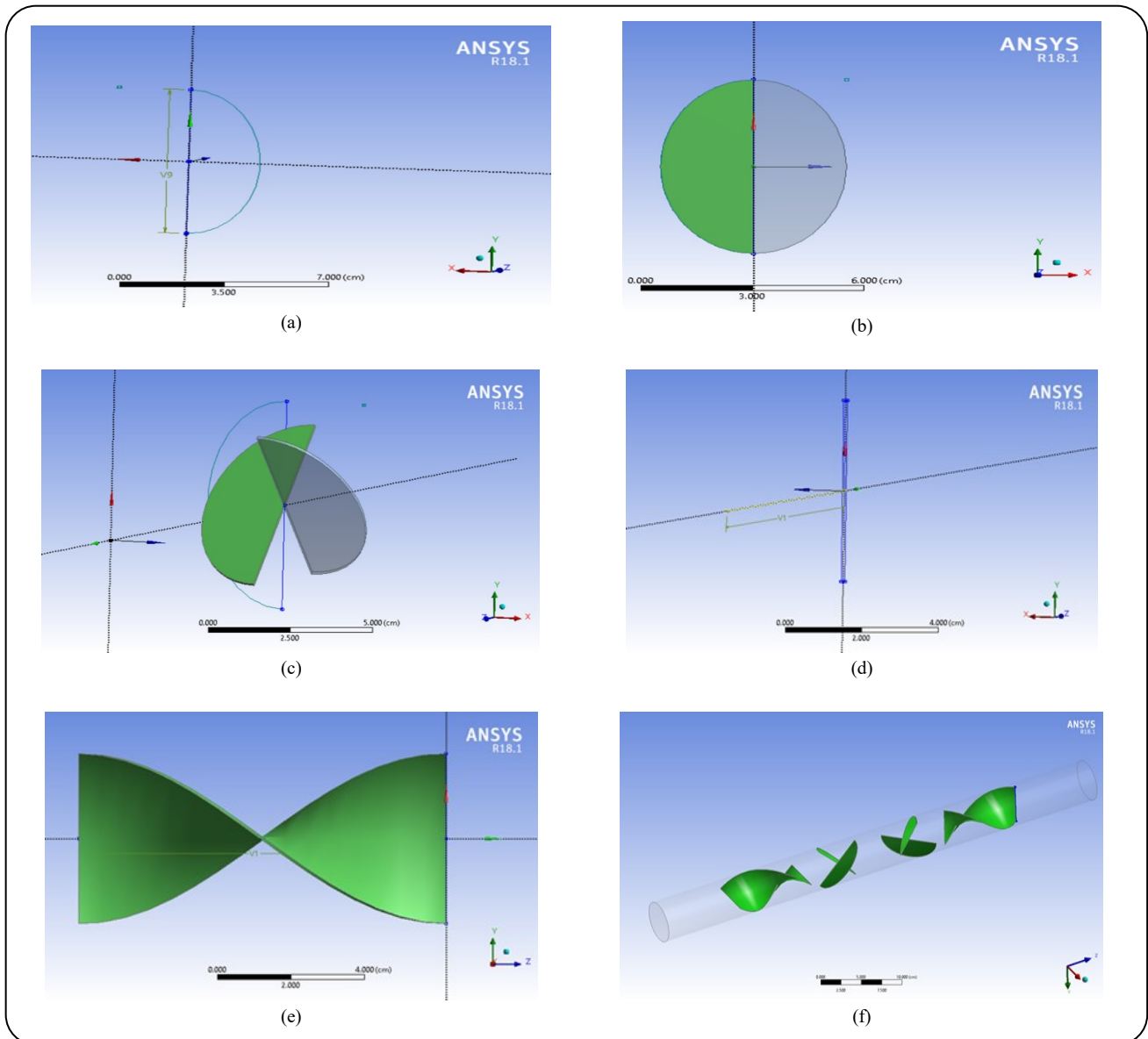
***Fig. 3: (a) Sketching semi-ellipse (b) Generating elliptical body (c) Rotating elliptical body (d) Generating rectangle
and line of twist (e) Generating twist (f) Formation of TEET design***

the twist details, it also twists the geometry along the reference line, as shown in Fig. 3 (e). After they were making both Kenics and LPD make a copy of both mixing elements and rotate both copies 90 degrees relative to the original one, and arrange them into a TEET pattern, then create a fluid domain around it as shown in Fig. 3 (f) [25, 26].

Governing equations

The principles on which the governing equations of fluid flow are based are; conservation of mass, momentum, and energy conservation. The application of principles to control volume results in continuity, momentum, and energy equations, respectively. The fundamental laws of conversation can be applied to both infinitesimal and finite control volume. The finite control volume yields Integral forms while the infinitesimal control volume yields partial differential equations; two reference frames are widely used to derive these equations, Eulerian and Lagrangian. However, the equations derived in the Eulerian frame of reference are directly obtained in the conservative form, suitable for numerical methods like the finite volume method. This research utilizes the same conservative forms

of governing equations in partial differential form, and the same will be implemented in the solver [23, 24]. Continuity equation the application of mass conservation on a control volume yields continuity equation which is as follows:

$$\frac{\partial \rho}{\partial t} + \nabla(\rho V) = S \tag{1}$$

The momentum equation arises due to the application of Newton's second law of motion. These equations are defined as:

$$x - \text{component: } \frac{\partial(\rho u)}{\partial t} + \nabla(\rho u V) = \tag{2}$$
$$-\frac{\partial p}{\partial x} + \frac{\partial \tau_{xx}}{\partial x} + \frac{\partial \tau_{yx}}{\partial y} + \frac{\partial \tau_{zx}}{\partial z} + \rho f_x$$

$$y - \text{component: } \frac{\partial(\rho v)}{\partial t} + \nabla(\rho v V) = \tag{3}$$
$$-\frac{\partial p}{\partial y} + \frac{\partial \tau_{xy}}{\partial x} + \frac{\partial \tau_{yy}}{\partial y} + \frac{\partial \tau_{zy}}{\partial z} + \rho f_y$$

$$z - \text{component: } \frac{\partial(\rho w)}{\partial t} + \nabla(\rho w V) = \tag{4}$$
$$-\frac{\partial p}{\partial z} + \frac{\partial \tau_{xz}}{\partial x} + \frac{\partial \tau_{yz}}{\partial y} + \frac{\partial \tau_{zz}}{\partial z} + \rho f_z$$

The energy equation is obtained by applying the conservation of energy equation on control volume. This equation is defined as:

$$\frac{\partial}{\partial t}(\rho E) + \nabla(V(\rho E + p)) = \nabla(k\nabla T) \tag{5}$$

where ρ=Density of fluid, V=Velocity field, S=Source term, p=Pressure, u,v,w=Velocity components in x, y, and z directions respectively, τ_{ij}=Stress components, f_i=Body force in i[th] direction, k=Thermal conductivity, E=Total energy of the fluid.

In the later part of the study, to access the mixing efficiency, the DPM analysis will be adopted. The DPM works on the Eulerian-Lagrangian approach. The fluid phase will be considered as a continuum, and Euler's frame of reference is considered. The particles will be considered in the Lagrangian frame. The particle exchanges momentum with the fluid phase [27, 28]. This approach is called Coupled DPM calculation. The momentum balance of particle yields:

$$\frac{du_p}{dt} = \frac{V - u_p}{\tau_r} + \frac{d(\rho_p - \rho)}{\rho_p} + F \tag{6}$$

Where $F = Source\ of\ momentum$

$$\tau_r = \frac{(\rho_p d_p^2)}{3\mu} \frac{4}{C_d Re} \tag{7}$$

$$Re = \frac{\rho d_p |u_p - u|}{\mu} \tag{8}$$

$$C_d = a_1 + \frac{a_2}{Re} + \frac{a_3}{Re^2} \tag{9}$$

These coefficients are pre-defined in the solver [22].

Assumptions

At this point in the study, assumptions are considered. As the working fluid is water, the density is assumed constant (incompressibility). As the static mixer geometry is horizontal, the body force of gravity is neglected. The fluid is Newtonian and steady-state conditions are assumed. No mass transfer mechanism into or out of the continuous phase is introduced at this study stage. Thus the source term in continuity becomes zero. No source of momentum is considered in fluid-particle interaction except drag. In the light of these assumptions, certain modifications are made in the governing equations, as follows. Continuity equation reduces to (by 1, 4, and 6).

$$\nabla.(V) = 0 \tag{9}$$

For Newtonian and incompressible fluids, the shear stresses are represented as:

$$\tau_{xx} = 2\mu \frac{\partial u}{\partial x} \tag{11}$$

$$\tau_{yy} = 2\mu \frac{\partial v}{\partial y} \tag{12}$$

$$\tau_{zz} = 2\mu \frac{\partial w}{\partial z} \tag{13}$$

$$\tau_{xy} = \tau_{yx} = \mu \left(\frac{\partial v}{\partial x} + \frac{\partial u}{\partial y} \right) \tag{14}$$

$$\tau_{xz} = \tau_{zx} = \mu \left(\frac{\partial w}{\partial x} + \frac{\partial u}{\partial z} \right) \tag{15}$$

$$\tau_{yz} = \tau_{zy} = \mu \left(\frac{\partial w}{\partial y} + \frac{\partial v}{\partial z} \right) \tag{16}$$

For Newtonian fluids, the resulting momentum conservation equations are called Navier Stokes equations which are given below. The given version of the Navier Stokes equation is the steady-state version [20, 21].

For x-component:

$$\rho\left(\frac{\partial(u^2)}{\partial x} + \frac{\partial(uv)}{\partial y} + \frac{\partial(uw)}{\partial z}\right) \tag{17}$$

$$= -\frac{\partial p}{\partial x} + \frac{\partial}{\partial x}\left(2\mu\frac{\partial u}{\partial x}\right) + \frac{\partial}{\partial y}\left[\mu\left(\frac{\partial v}{\partial x} + \frac{\partial u}{\partial y}\right)\right] +$$

$$\frac{\partial}{\partial z}\left[\mu\left(\frac{\partial w}{\partial x} + \frac{\partial u}{\partial z}\right)\right]$$

For y-component:

$$\rho\left(\frac{\partial(uv)}{\partial x} + \frac{\partial(v^2)}{\partial y} + \frac{\partial(vw)}{\partial z}\right) \tag{18}$$

$$= -\frac{\partial p}{\partial y} + \frac{\partial}{\partial x}\left[\mu\left(\frac{\partial v}{\partial x} + \frac{\partial u}{\partial y}\right)\right] + \frac{\partial}{\partial y}\left[2\mu\left(\frac{\partial v}{\partial y}\right)\right] +$$

$$\frac{\partial}{\partial z}\left[\mu\left(\frac{\partial w}{\partial y} + \frac{\partial v}{\partial z}\right)\right]$$

For z-component:

$$\rho\left(\frac{\partial(uw)}{\partial x} + \frac{\partial(vw)}{\partial y} + \frac{\partial(w^2)}{\partial z}\right) \tag{19}$$

$$= -\frac{\partial p}{\partial z} + \frac{\partial}{\partial x}\left[\mu\left(\frac{\partial w}{\partial x} + \frac{\partial u}{\partial z}\right)\right] + \frac{\partial}{\partial y}\left[\mu\left(\frac{\partial w}{\partial y} + \frac{\partial v}{\partial z}\right)\right] +$$

$$\frac{\partial}{\partial z}\left[2\mu\left(\frac{\partial w}{\partial z}\right)\right]$$

At the initial stage, the interest of the study lies in determining pressure and velocity fields in the domain. The following boundary conditions are assumed; the inlet is chosen to be a velocity inlet.

$$V = -U_o\hat{k} \tag{20}$$

The no-slip condition is applied to the wall. The outlet is considered a pressure outlet.

Mesh development

Before making a fine mesh, generate a default mesh to determine the sections where mesh refining is needed. After generating the default mesh, select tetrahedron as the mesh method because it is suitable for unstructured meshing. Since the need to capture the gradients of both the velocity and pressure close to the mixing elements. It needs a very refine mesh near them. The addition of advanced sizing function and setting refinement to proximity and curvature refine the mesh near all curve surfaces and narrow pathways, as you can see in Fig. 4 (a, b). Quality of generated mesh; orthogonal quality 0.7 (average), skewness 0.3 (average), statistics 919993 nodes and 4421587 elements [12, 19].

The solver setup for the first part deals with the single-phase flow inside the static mixture and the second part deals with the multi-phase flow.

RESULTS AND DISCUSSION
Pressure drop and thermal analysis

In pressure drop analysis, a pressure-based solver was used. It applies to a wide range of flow regimes, such as incompressible slow-speed flows. In a pressure-based solver, the velocity field is obtained from the momentum equation, and the pressure correction equation solves continuity, pressure velocity coupling algorithms. It is derived by reformatting the continuity equation, and the pressure equation is derived so that the velocity field corrected by the pressure satisfies continuity. The governing equations are nonlinear and coupled to one another. The solution process involves iterations wherein the entire governing equations are solved repeatedly until the solution converges. Pressure-based solver has two algorithms which include segregated and coupled algorithms, use the coupled algorithm in simulation. In a coupled algorithm, each governing equation is not solved one after another like it was in a segregated algorithm, unlike it solves a coupled system of equations is shown in Fig. 4 (c). The coupled algorithm solves the momentum and pressure-based continuity equations together. The remaining equations are solved one after another as it was solved in the segregated algorithm.

First, it updates the fluid properties like density and viscosity. Then it solves the momentum and pressure-based continuity equation simultaneously. Then pressure correction equation is solved with the help of velocity field and mass flux. Equations are solved for additional scalars like energy, species, and radiation intensity using the current values of the solution variables, and these steps are repeated until convergence is achieved. The coupled algorithm is slightly more computationally expensive than a segregated algorithm because the momentum and continuity equations are stored in the memory while solving for pressure and velocity field. But it gives more robust results and is efficient in solving single-phase flows in steady-state conditions. On top of that, it solves continuity and momentum equations in a coupled manner, so the rate of solution convergence is increased [16, 17].
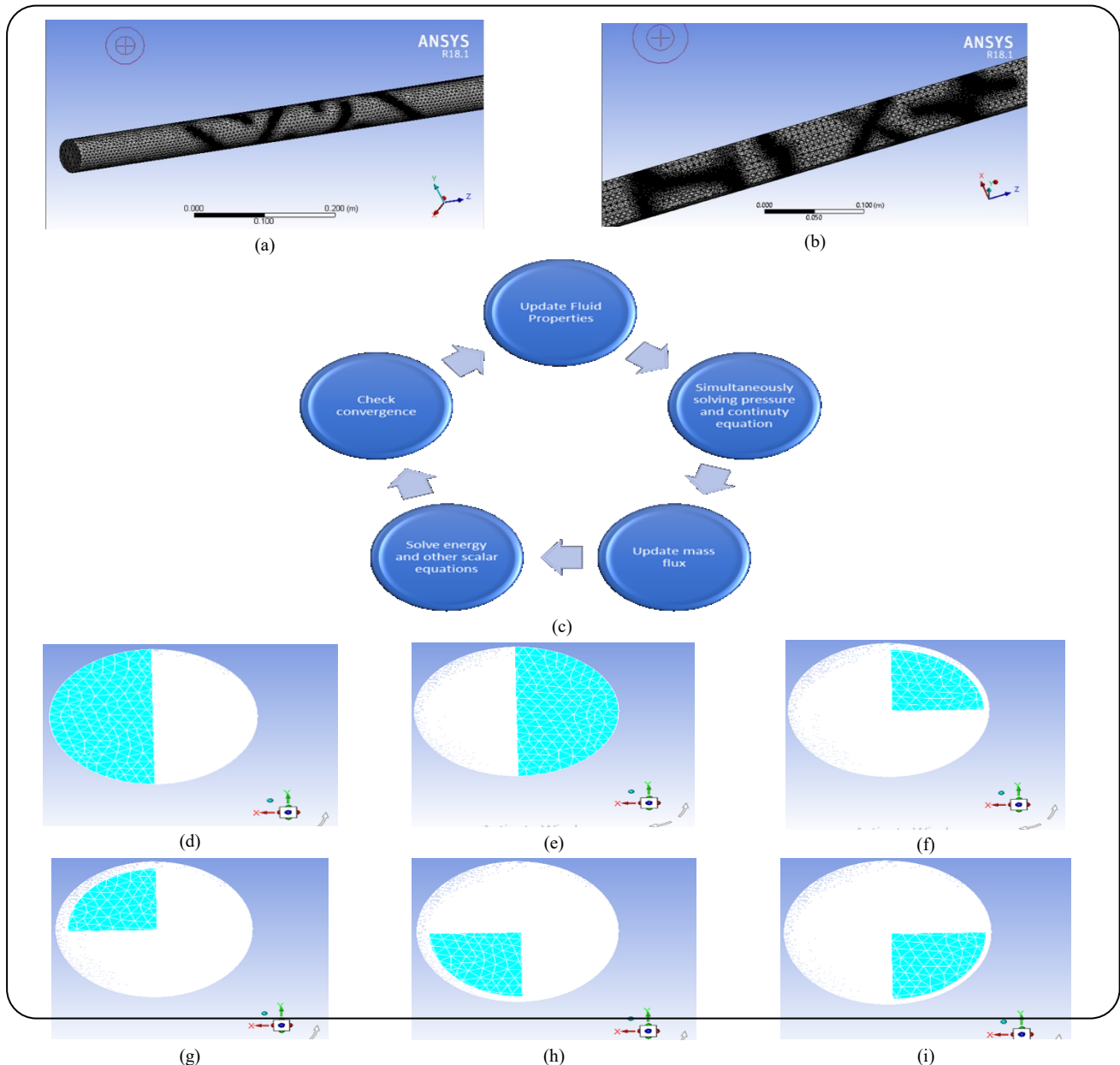
Fig. 4: (a) Meshed geometry (b) Meshed elements (c) Coupled algorithm (d) Injection of particles on the left side (e) Injection of particles on the right side (f) For 1st quarter sampling plane 1 (g) For 2nd quarter sampling plane 2 (h) For 3rd quarter sampling plane 3 (i) For 4th quarter sampling plane 4.

Velocity formulation and model

For the case, absolute velocity formulation is applicable because it is valid for flows. A large part of the domain is not rotating and already selects a coupled solution algorithm. Hence, relative velocity formulation is not compatible with it. Steady-state Laminar flow was considered for both. In addition, the energy equation was enabled for the thermal analysis to calculate the thermal profile of the fluid [14, 15].

Cell zone conditions

Fluent's database offers a wide variety of material for working. The Fluent database offers six types in general, such as solids, fluids, mixtures, combusting particles, inert particles, and droplet particles. Since the case required only to specify the fluid for fluid domain hence, selected the water-liquid from Fluent's fluid database which properties are density = 1000 kgm^{-3}, Heat Capacity = 4182 J/kg K, Thermal Conductivity = 0.6 W/K m, and viscosity = 0.001 kg/m sec at 20ºC.

Boundary conditions

To reduce the simulation's complexity and time, set up a simulation for an empty pipe equal to the entrance length of the corresponding Reynolds number. The fully developed velocity profiles were thus obtained. At the mixer's inlet, those velocity profiles were read to ensure a fully developed profile before interacting with the mixer elements. The mixer's outlet was set up as a pressure outlet, and the wall of the pipe and the mixer elements are treated as the stationary wall. No-slip condition is applied to all the walls. For thermal analysis, a constant heat flux of 500 W/m^2 is introduced through the pipe wall to study the thermal energy transport in the mixer [13].

Spatial discretization

For the gradient, use the least square cell-based method. This method calculates the face value as an average of the two adjacent cells having a common face. This averaging assumes equal contribution from both cells regardless of their geometric properties like skewness. It is the least accurate but computationally cheaper than the other methods. Select the second-order upwind scheme for pressure, momentum, and energy because it gives accurate results than the first-order upwind technique. Second-order upwind uses upstream values to evaluate the property on the boundaries of the cell and then uses them to compute the value at the center of the cell.

Pseudo transient

Pseudo transient is a form of implicit under-relaxation for steady-state cases. It helps in stabilizing the case and, at the same time, give faster convergence. In the pseudo transient method, an artificial transient term is added to the equation's equation. It allows the solution to march forward in "time." However, since the flow is steady, the transient variations go away when convergence is reached, and the steady-state solution is recovered.

Solution controls

Flow Courant number is set to 200. Courant number is the ratio of the distance the flow moves across the cell and the length. The larger the time, the step farther the flow moves across the cell. Courant Number is used to stabilize the convergence behavior. The larger value of the courant number is not acceptable for explicit methods. In solving a set of nonlinear equations, it is necessary to control the change of discrete values of the scalar. It is typically achieved by explicit relaxation, which reduces the change during each iteration. In a simple form, the new value of the variable within a cell depends upon the old value, the computed change in a scalar variable, and the under-relaxation factor, which is called alpha. Explicit relaxation factors set in are; momentum 0.5 and pressure 0.5 [18].

Hybrid initialization

In steady simulations, the initialization should not impact the final converged solution. It only affects the number of iterations to reach it. Hybrid initialization is based on the solving of Laplace's equation to determine the pressure and velocity parameters. Other parameters like temperature and frictions have been taken as per the standard program. Hence analysis is independent of the environmental parameters, so use hybrid initialization in case.

For Multiphase Analysis

The mixing in the static mixer uses Discrete Phase Model-DPM in which the continuous phase is liquid-water, and the discrete phase is solid particles. After solving continuous phase transport equations, simulated the 2nd phase in the Lagrangian frame of reference. The discrete phase consists of solid particles having a spherical shape. In the simulation, water is the dispersing medium, and solid particles are the dispersed phase. DPM account for dispersed- continuous interaction with low volume loading. Trajectories of these particles are calculated by solving the balanced equation for momentum. The coupling between the discrete phase and continuous phase and its impact on both phases are computed. First, solve the continuous flow field by the solver setup described above for pressure analysis. Two planes are made at the mixer's inlet for injecting particles, as shown in Fig. 4 (d, e). Then for sampling, four planes are created, or the pipe cross-section is divided into four quarter circles to take four samples after the inlet and just before the mixer's outlet, as mention in Fig. 4 (f, g, h, i).

The 2-injections are made, one for the left and one for the right plane, and 1e-4 m diameter particles are injected from these surfaces with the velocity of 0.01 m/sec normal to flow field. The interaction with the continuous phase is enabled. Trajectories of discrete phase solid spherical particles are predicted by integral force balance on these particles, equating the particle inertia with force acting

on a particle. In solver, decrease the continuity residual, and without initializing the solution, the calculation is run for particle trajectories, and the particle trajectories are observed using graphs and particle tracing graphics [11].

Validation of CFD simulation

After convergence, the results are obtained. It ensures that results represent the actual physical phenomenon and support actual evidence; validation is required. There remain some aspects of the physical problem which are missed while developing the mathematical model. The validation assesses these shortcomings. There must be a certain level of consensus in both the simulation results and actual findings for a simulation to be successful. There are multiple methods to validate the mathematical model. The primary one is comparing with experimental data. In the absence of this, data from sources that closely resemble the physical problem can be used. Also, the trends and sensitivities of process variables can be compared with the established results and standards. Since working on the novel static mixer geometries, I used the second and third options to validate the model [10]. Apart from the model, the numerical solution is dependent on the grid. The resolution and geometrical aspects of the solution grid do influence the final solution. Since the errors of the numerical methods are proportional to the size of the grid, to achieve consistent results independent of the grid used, an optimum size is required. The process of finding the optimum size is called GRID independence test [9].

Grid independence test

A grid independence test is performed on CFD simulation for validation. In this test, gradually refine mesh from course to fine and then see if there is any significant variation that occurs in the output parameters or not. The mesh size at which the variables die out and no significant observed change is chosen as the optimum size. The constraints in this optimization process are the computational expense, the accuracy of the final solution, and the end usage of the model. So, this 'significant variation' is relative and differs from model to model [7, 8].

To carry out the GRID independence test, set up a parametric analysis. It is a very convenient way to observe input-induced changes in output. The mesh size itself is affected by several parameters, including max face size, min size, growth rate, and proximity size. Considering the curvature and complex zones in the geometry, choose the proximity size as a key input parameter for the GRID test. Three outlet variables were chosen to monitor the results, named outlet velocity, outlet pressure, and inlet pressure. All three were area-averaged quantities. The minimum proximity size was varied from 0.9 to 0.5 mm. The smaller size creates more cells and nodes; thus, refinement of the mesh takes place. However, the computational requirements also increase with it [5, 6]. As evident in Fig. 5 (a, b, c), after refining mesh to a very large extent, the variation in velocity and pressure parameters are 1e-4 m s^{-1} and 1e-3 Pa, respectively, which is negligible. Chose 0.85 mm as the optimum size to work out the simulation without excessive processing capabilities and good engineering accuracy [4].

Validation by literature pressure drop analysis

Pressure drop is one of the important parameters in assessing the performance of inline mixers in the industry. In literature, the pressure drop for the static mixer is represented by a factor called Z-factor, which is the ratio of pressure drop through the mixer to the pressure drop through the empty pipe of the same length as the inline mixer. Use the same terminology in the case and compared Z factors with that of literature. For Kenics and LPD mixers, there are several correlations available, but they are solely for their single geometry variants. For hybrid combinations of LPD and Kenics, no such correlation is available in the literature. Based on the single geometry variants, the correlation contains various parameters like the arrangement of the elements, their aspect ratio, and the flow regime. In hybrid geometry, no such unique geometrical parameters can be deduced due to different mixer elements [2, 3].

The model is thus validated by comparing the trend of the Z factor versus the Re number. In all single geometry variants of Kenics and LPD, Z factor versus Re is linear. Similarly, the case simulated yielded the same linear relationship between the Z factor and the Re number. Fig. 5 (d) confirms the validity of the velocity and pressure field calculated. The literature sources for the correlations are provided Z = 5.4+0.028, Re = 1.36, *Cyubulski* and *Werner* (1986) and Z = 5.34+0.0211, Re = 2, *Sir* and *Lecjaks* (1982). The aspect ratio of the twisted element in the standard case is 2, so used the "*Sir* and *Lecjaks* (1982)" correlation and found that the mixer shows the traditional linear behavior as stated in literature data [27, 28].

Table of Design Points					▼ ⊡ X
	B	C	D	E	F
1	P3 - Mesh Proximity Min Size ▼	P2 - Mesh Elements ▼	P4 - inlet-pressure ▼	P5 - outlet-velocity ▼	P6 - total pressure at outlet
2	mm ▼		Pa	m s^-1	Pa
3	0.9	9.1224E+05	0.88172	0.0096214	0.050151
4	0.85	9.8843E+05	0.88137	0.0096245	0.050145
5	0.8	1.0838E+06	0.88023	0.0096203	0.050185
6	0.75	1.1885E+06	0.88057	0.0096142	0.050247
7	0.7	1.3119E+06	0.88068	0.0096318	0.050432
8	0.65	1.4599E+06	0.88164	0.0096303	0.050352
9	0.6	1.6397E+06	0.88285	0.0096333	0.050343
10	0.55	1.8567E+06	0.88332	0.0096513	0.050328
11	0.5	2.1223E+06	0.88377	0.0096352	0.050458
*					

(a)

(b)

(c)

(d)
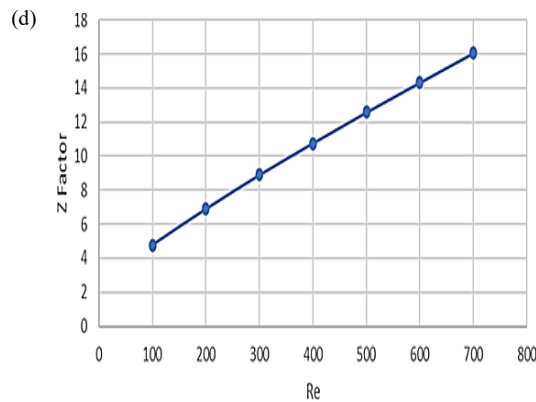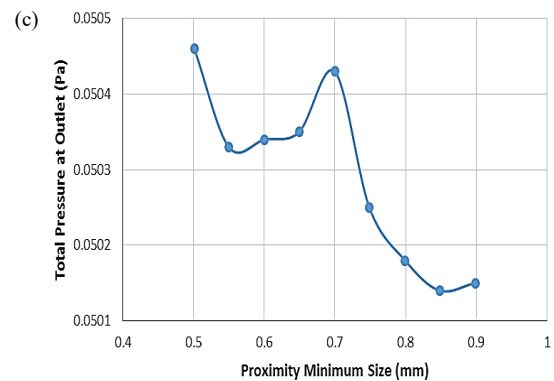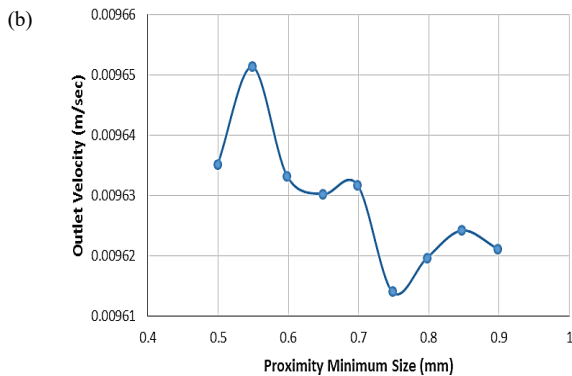
Fig. 5: (a) Grid Independence test results (b) Mesh Proximity minimum size versus outlet velocity (c) Mesh Proximity minimum size versus total outlet pressure (d) Re versus Z Factor of standard 90° LPD.

To observe the mixing efficiency of mixer designs, we have calculated the Relative Standard Deviation (RSD) percentage value, compared the RSD value of the standard 90° case with the RSD value that exists in the literature. The greater the RSD% lesser would be the mixing performance, while the lower the RSD %, the greater the mixing efficiency. Referring to the Bunkluarb *et al.* data,

the RSD value for the standard 90° case was calculated as 20.32%. However, the simulated result gives a better result; the RSD value obtained is 13.538% showing better mixing than the literature data. It is due to the difference in physics involved, like wall-fluid interactions. In the research, article walls were imposed with the Slip Condition. However, for the more realistic result, it has

assumed the widely acclaimed "No-Slip Condition" at the wall-fluid interface [7, 21]. Though there is complete agreement in geometry in both cases, the Reynold number was different due to fluid properties. Also, it considered the horizontal flow; thus, no effect of gravity was present in the case, while the research article used a vertical flow pattern. Thus, there might be a difference in particle dynamics in DPM analysis.

Post-processing

A total of nine cases were simulated, and each case was run for a total of eight different Reynold's numbers. For each case, pressure drop analysis, thermal analysis, and DPM were performed to help conclude the best mixer geometry in mixing efficiency, pressure drop, and heat transfer coefficient. The CFD solver yields just the values of velocity, temperature, and pressure at each domain cell. The rest of the quantities of interest are obtained using post-processing. CFD post-processing extracts the numerical results from the solution, evaluates the dependent quantities like shear, gradients and presents them in graphical, easy to infer forms such as contours, surface plots, animations, streamlines, particle tracking, data charts.

Pressure drop analysis

The pressure drop analysis was performed in terms of Z-factor, the ratio of pressure difference in the static mixer to pressure difference in the empty pipe. An empty pipe was designed for laminar flow, and the simulation was run for all eight selected Reynold's numbers to obtain results for the pressure drop in an empty pipe. The pressure drop is the difference in static pressure at the inlet to that at the outlet. The pressure contours are obtained at the inlet, outlet, and four interior planes in the mixer [24]. Fig. 6 (a) shows the Re versus Z factor for standard TEET 90°, 100°, 110°, and 120°. The four interior planes introduced after each mixing element and the inlet and outlet where the velocity and pressure contours are obtained can be visualized in Fig. 6 (b). Fig. 6 (c) shows the Re versus Z Factor of curved edge Kenics 90° and 120°. Fig. 6 (d) also shows the inlet, outlet, and interior planes of curved edge Kenics 120°. Fig. 6 (e) shows the modified aspect ratio Kenics 90° and 120°. Fig. 6 (f) inlet, outlet, and interior planes of modified aspect ratio Kenics 120°. Fig. 7 (a) shows the velocity, and Fig. 7 (b) shows the pressure contours for standard TEET mixers.

Fig. 7 (c) shows the velocity, and Fig. 7 (d) shows the pressure contours for curved edge Kenics mixers. Fig. 7 (e) shows the velocity, and Fig. 7 (f) shows the pressure contours of modified aspect ratio Kenics.

Thermal analysis

It performs thermal analysis, the energy equation was enabled in the solver, and a constant heat flux value of 500 W/m^2 was introduced at the pipe wall. The solution was iterated until it converged. The fluent reports provided the values of wall temperature (T_w) and bulk temperature (T_b), used to calculate the heat transfer coefficient. Like pressure, temperature contours are also obtained at six planes in the mixer [10]. Fig. 8 (a) shows the Re versus heat transfer coefficient of standard TEET mixer 90°, 100°, 110°, and 120°. Fig. 8 (b) shows the Re versus heat transfer coefficient of curved edge Kenics mixer 90° and 120°. Fig. 8 (c) shows the modified aspect ratio Kenics 90° and 120°.

$$h = \frac{q}{(T_w - T_b)} \tag{21}$$

Fig. 9 (a) shows the temperature contours of standard TEET mixers. Fig. 9 (b) shows the temperature contours of curved-edged Kenics mixers. Fig. 9 (c) shows the temperature contours of modified aspect ratio Kenics mixers.

Discrete phase model (DPM)

In the DPM, anthracite particles of uniform diameter 0.0001m having a density of 1550 Kg/m^3 with velocity magnitude and total flow rate of 0.01 m/sec and 1e-20 Kg/sec, respectively, are injected through the left. The outlet boundary condition was defined as escape and the walls were set to reflect the particles. The samples were analyzed by counting the number of particles falling in a sample from each injection.

Then, the fraction was calculated for the right injection by calculating the number of particles from the right injection to the total number of particles in a sample. The calculated sample fraction is used to calculate standard deviation, converted into relative standard deviation (RSD) by dividing it with the sample mean. The final step is to plot the particle distribution for which the data was sorted and plotted using the python-based package [15, 26]. Fig. 10 (a, b, c, d, e) shows the standard TEET particle distribution of 90°, 100°, 110°, and 120°. RSD values
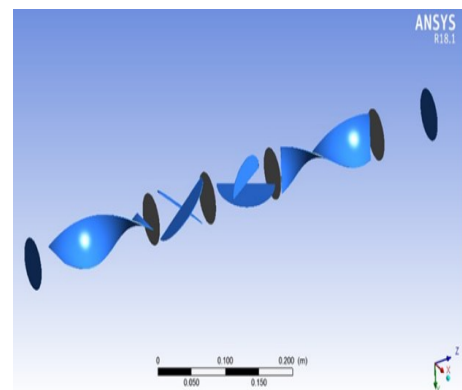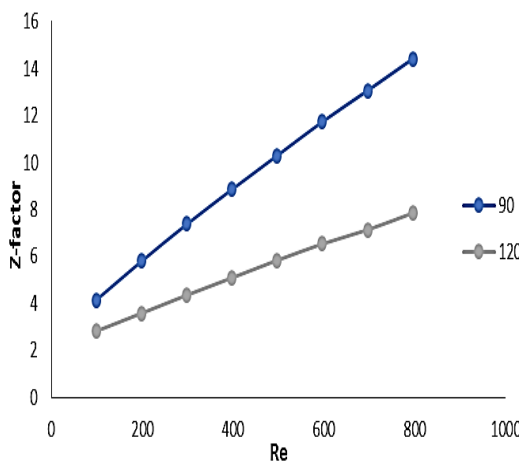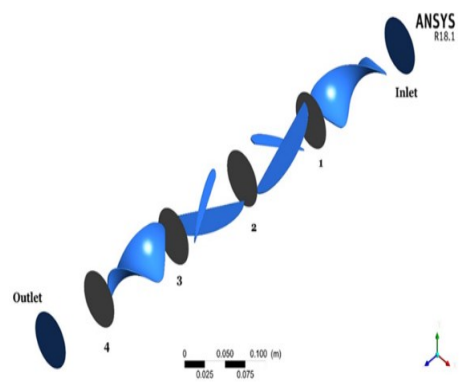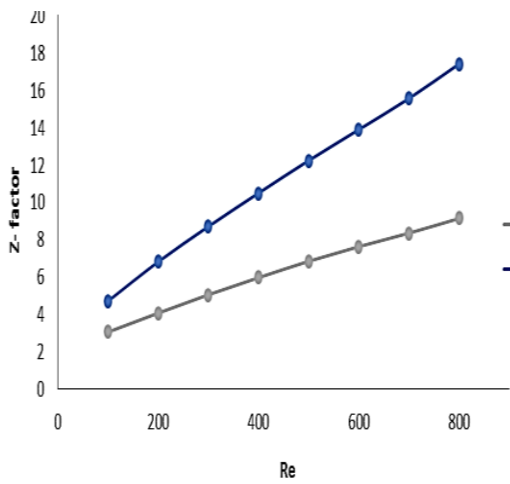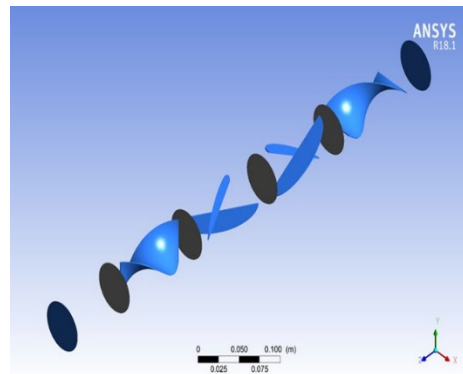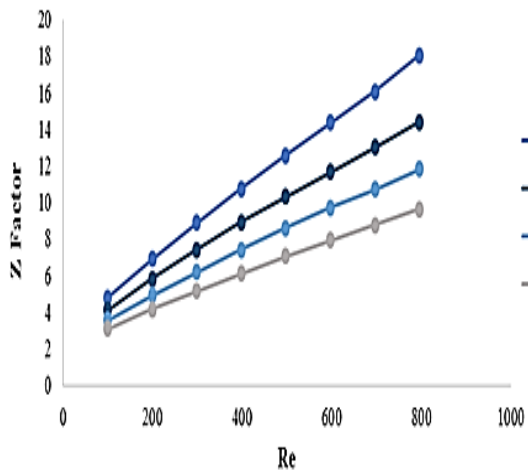
Fig. 6: (a) Re versus Z factor for standard TEET (b) inlet and outlet at which the velocity and pressure contours (c) Re versus Z Factor for curved edge Kenics 90º and 120º (d) Inlet, outlet, and interior planes of curved edge Kenics 120º (e) Re versus Z Factor of modified aspect ratio Kenics 90º and 120º, (f) Inlet, outlet and interior planes of modified aspect ratio Kenics 120º.
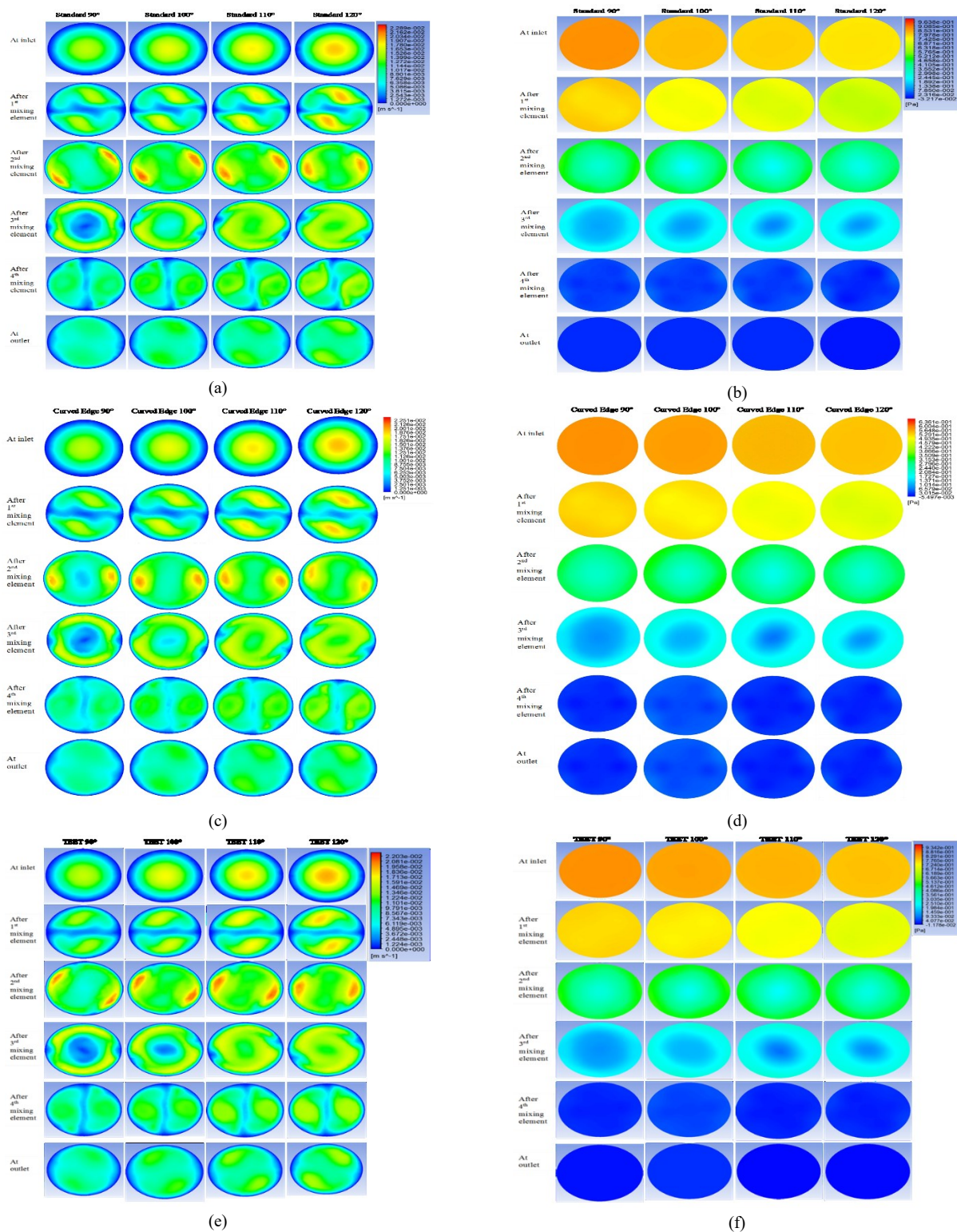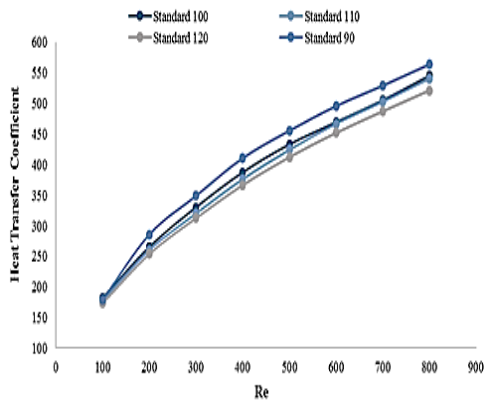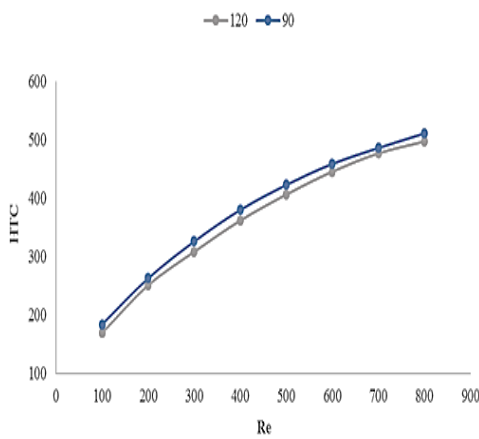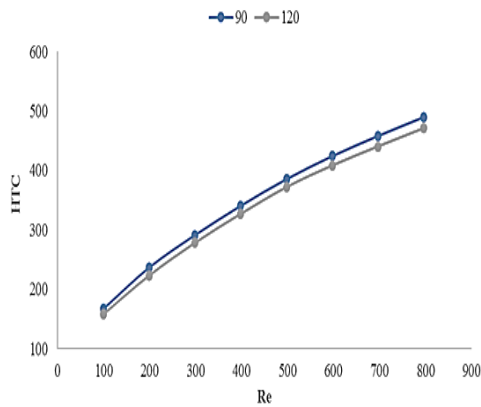
         Research Article

Fig. 7: (a) Velocity contours for standard TEET mixers (b) Pressure contours for standard TEET mixers (c) Velocity contours for curved edge Kenics mixers (d) Pressure contours for curved edge Kenics mixers (e) Velocity contours of modified aspect ratio Kenics (f) Pressure contours of modified aspect ratio Kenics.

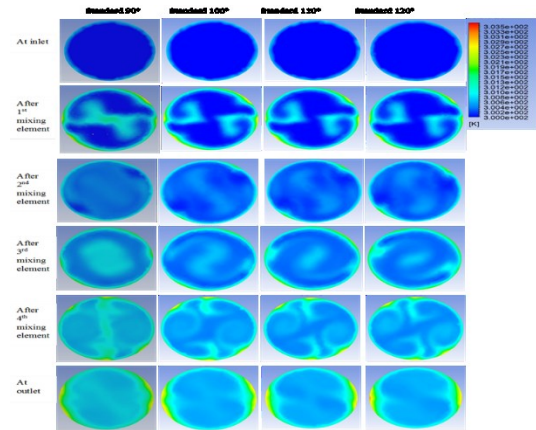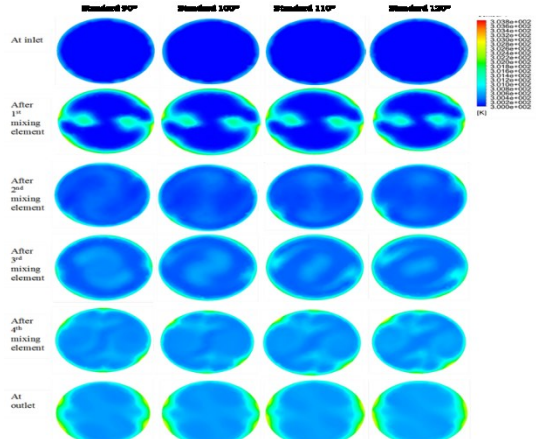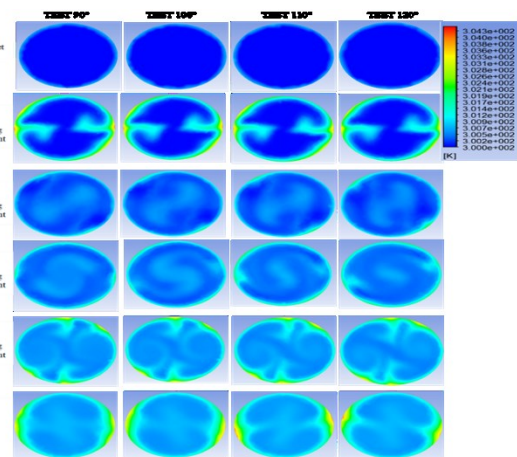(a)

(b)

(c)

(a)

(b)

(c)

Fig. 8: Re versus heat transfer coefficient (a) standard TEET mixer 90º, 100º, 110º, and 120º (b) curved edge Kenics mixer 90º and 120º (c) Re versus heat transfer coefficient of the modified aspect ratio Kenics mixer 90º and 120º.

Fig. 9: (a) Temperature contours of standard TEET mixers (b) Temperature contours of curved edged Kenics mixers (c) Temperature contours of modified aspect ratio Kenics mixers.
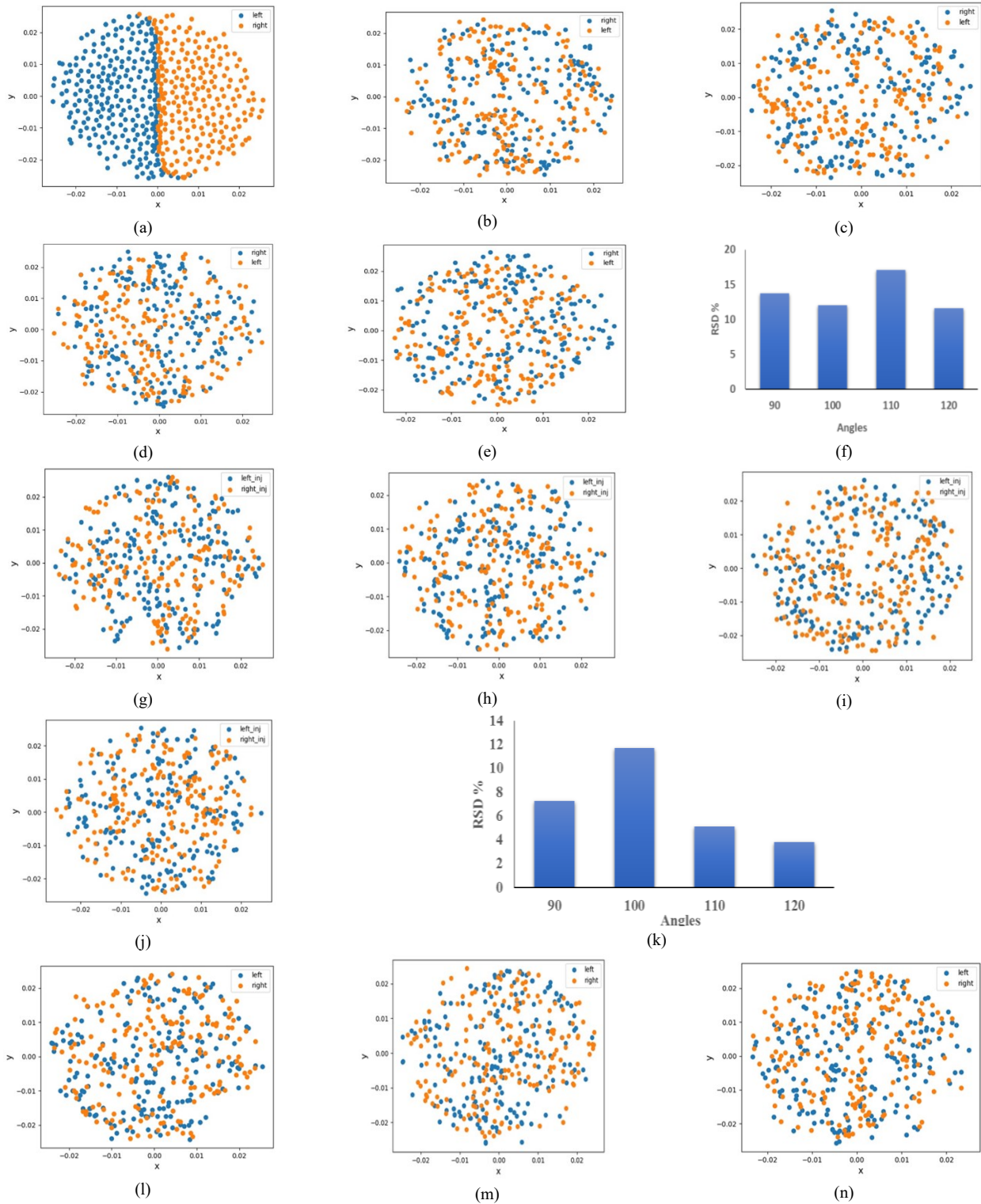
Fig. 10: Standard TEET particle distribution (a) Inlet 90º (b) Outlet 90º (c) Outlet 100º (d) Outlet 110º (e) Outlet 120º (f) RSD values for standard TEET variants. Curved edged Kenics particle distribution (g) Outlet 90º (h) Outlet 100º (i) Outlet 110º (j) Outlet 120º (k) RSD values for curved edge variants. Modified aspect ratio Kenics particle distribution (l) Outlet 90º (m) Outlet 100º (n) Outlet 110º (o) Outlet 120º (p) RSD values for modified aspect ratio variants.

(o)

(p)

Fig. 10: Standard TEET particle distribution (a) Inlet 90º (b) Outlet 90º (c) Outlet 100º (d) Outlet 110º (e) Outlet 120º (f) RSD values for standard TEET variants. Curved edged Kenics particle distribution (g) Outlet 90º (h) Outlet 100º (i) Outlet 110º (j) Outlet 120º (k) RSD values for curved edge variants. Modified aspect ratio Kenics particle distribution (l) Outlet 90º (m) Outlet 100º (n) Outlet 110º (o) Outlet 120º (p) RSD values for modified aspect ratio variants. (Continues)
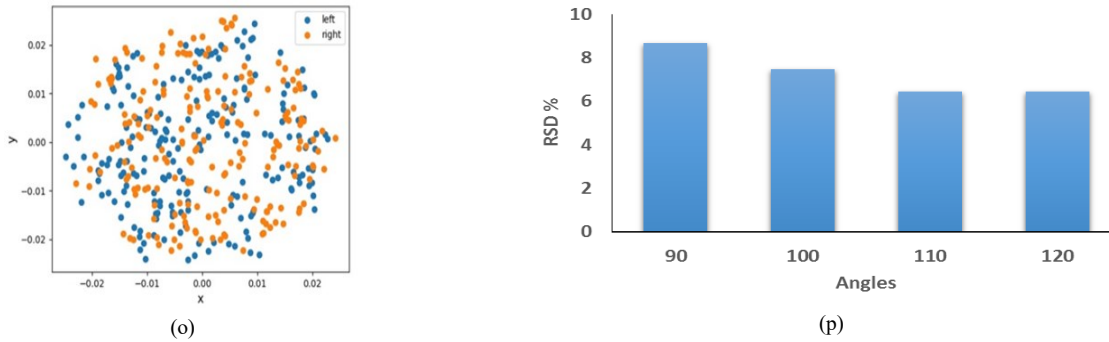
for standard TEET variants are shown in Fig. 10 (f). Fig. 10 (g, h, i, j) shows the curved-edged Kenics particle distribution of 90º, 100º, 110º, and 120º. RSD values for curved edge variants are shown in Fig. 10 (k). Fig. 10 (l, m, n, o) shows the modified aspect ratio Kenics particle distribution of 90º, 100º, 110º, and 120º. RSD values for modified aspect ratio variants are shown in Fig. 10 (p).

The geometries built for analysis were classified into three groups as shown in Fig. 11 (a), the standard TEET geometries with four different angles (90º, 100º, 110º, 120º), the curved edged Kenics with two angles (90º and 120º), and the modified aspect ratio of Kenics with two angles (90º and 120º). Pressure drop analysis, thermal analysis, and DPM were run on all the cases, and the results are compared to conclude the best working geometry. First, the comparison is made based on the angle in the same group, and lastly, a joint comparison is made for all the groups as shown in Figs. 11 (b, c) [18, 19].

Curved edge geometry comparison

It observed the promising performance of curved edge mixers in pressure drop and heat transfer; a separate study was conducted for curved edge 120º with different blend radii for the same range of Re numbers. Three different blend radii were considered, which are 0.5, 1.0, and 1.5 cm, respectively is shown in Fig. 11 (d, e) [5]. There are two key parameters for mixer pressure and mixing efficiency, and there is a trade-off between them. The pressure drop was accessed using the widely used Z factor. The mixing efficiency was observed using two schemes; heat transfer analysis was done. The dispersive mixing characteristics observed in distributive mixing were

analyzed using DPM [7, 20, 21]. Pressure drop analysis reveals that standard geometries have the highest Z factor than their variants in curved edge and modified aspect ratio mixers. Also, while increasing the angle, there is a successive decrease in the Z factor; hence, the LPD angle of 90º gives the highest pressure drop while 120º gives the lowest.

Furthermore, the modified aspect ratio mixers give the lowest Z factor amongst all for every angle. This behavior requires special attention as the length of Kenics in this geometry is larger than the curved edge and standard Kenics element. This increased length certainly contributes to the increased wall shear, and hence, more pressure drop should be expected. However, by careful examination, it was found out that the less intense rotation of fluid around the axis in long Kenics compared to standard one results in a low-pressure drop across the mixing element. In long Kenics, the fluid is given the same 180º rotation around the axis slower than the standard case. It results in less intensive mixing and more undisturbed flow hence less pressure drop. Thus, it can be concluded that this reduction in pressure drop outnumbers the increased wall shear and skin friction resulting in low Z factors for modified aspect ratio. The curved edge geometry gives low Z factors than standard geometries, and the difference between the two becomes more prominent at higher Re numbers. These geometries have filleted edges of the Kenics element. These edges resulted in less flow resistance and less pressure drop across the mixer [8, 15].

In heat transfer analysis, dispersive mixing was analyzed. It was revealed that the standard cases give the best heat transfer performance, curved edge competes well
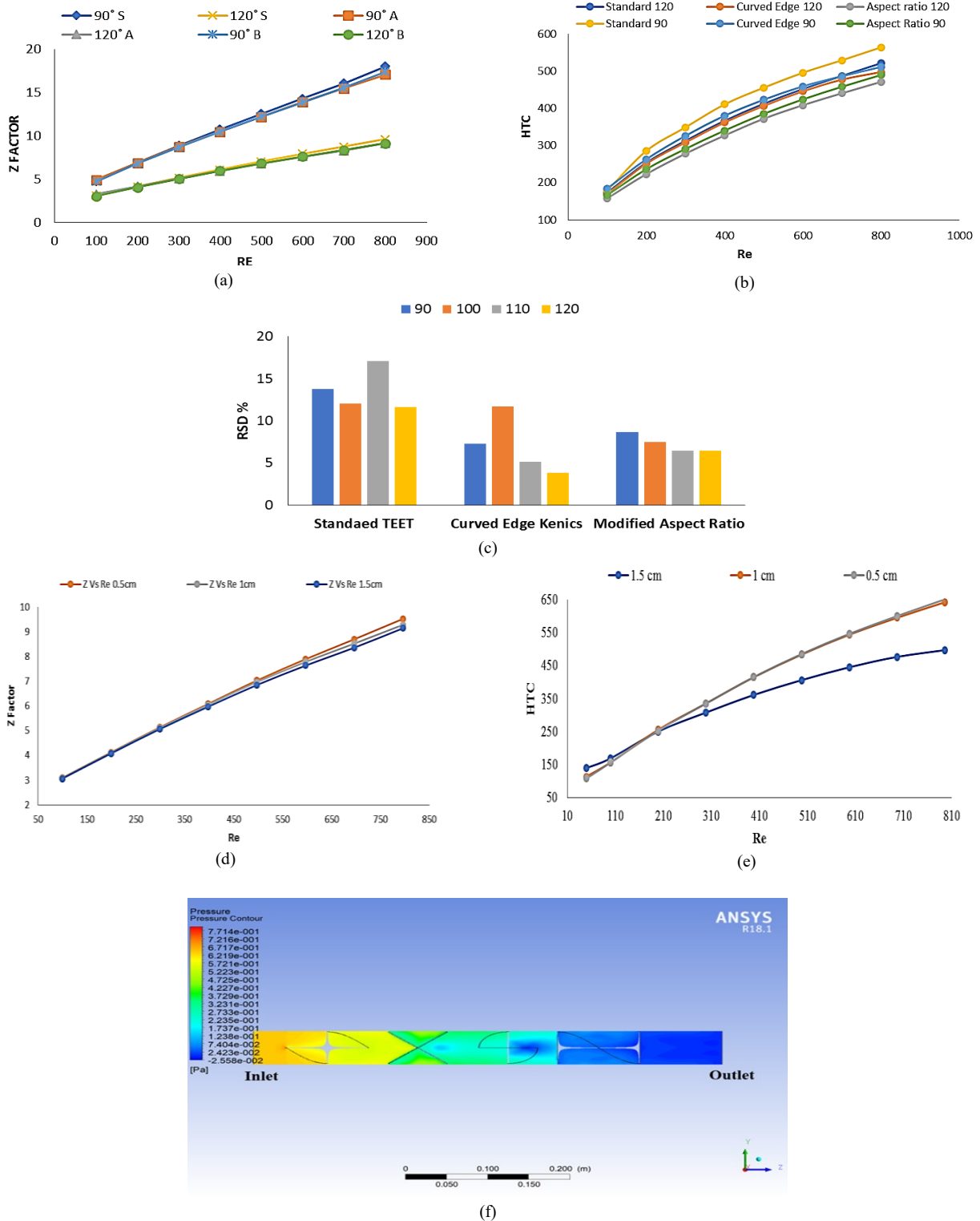
(a)

(b)

(c)

(d)

(e)

(f)

Fig. 11: (a) Re versus Z factor of all modified TEET geometries (b) Re versus HTC of all modified TEET geometries 90° and 120° (c) Comparison of DPM static mixer 90°, 100°, 110°, 120° (d) Re versus Z factor of different blend radius of curved edge geometry 120° (e) Re versus HTC of different blend radius of curved edge geometry 120° of heat flux 500 W/m² (f) Pressure profile through the length of the static mixer

with good HTCs while modified aspect ratio mixers give lowest HTCs. Moreover, increasing the LPD angle gives decreasing heat transfer coefficients. The angle of 90° gives a fairly high HTC compared to 120°, and this trend continues in all three classes of geometries. However, the difference between HTCs of 90° and 120° for standard geometries becomes increasingly wide for Re number. Hence at a higher Re number, the mixing performance of Standard 90° improves remarkably. It indicates that some turbulence might be present in the standard 90° resulting in more pressure drop but enhanced mixing [20].

For the laminar regime in pipe flows, for constant heat flux from the wall, the Nusselt number and HTC are constant concerning Re number. However, in all the examined cases of mixers, there is an improvement in heat transfer with increasing Re number. It proves the excellent advantage of using static mixers for heat transfer applications. Another important finding is that the HTCs of the standard and curved edges are close. The difference increases with increasing Re number though with different rates in 90° and 120°. In 90°, it was observed that after the Re number of 100°, the curved edge dominates the standard's performance, while in 120°, the curved edge maintains good proximity with the standard's performance. It can be said that the curved edge will thus dominate the standard case in dispersive mixing at low Re numbers. The possible enhancement of performance in standard cases at moderate Re numbers is well explained by the increased mixing intensity due to sharp and blunt geometry, which might give rise to local turbulent eddies. However, at low Re numbers, these local eddies die out, and a curved edge becomes a promising option.

In the separate study on different radii of curved edge 120° due to the promising performance, the lowest pressure drop was observed for a blend radius of 1.5 cm. In comparison, the highest pressure drop was observed for 0.5 cm. The difference between the pressure drop is less at small Re numbers and becomes more pronounced at higher Reynolds numbers. It can be concluded hence that the advantage of using larger blend radii is best realized at high Re numbers. In heat transfer analysis, high heat transfer coefficients were obtained for radii of 0.5 and 1.0 cm. The difference between 0.5 and 1.0 cm is less than 0.5 and 1.5 cm. The difference increases with the Re number, however, at a greater rate than the Re versus Z factor curve. At low Re numbers, the difference becomes negligible,

and finally, after a Re number of 200, inversion happens. The HTC of 1.5 cm becomes greater than 0.5 cm. Hence, it is concluded that 1.5 cm or greater curved edge geometries supersede low radii at low Re numbers for the same amount of pressure drop [3, 22].

Finally, discrete particle analysis was used to access the distributive mixing efficiencies of mixers. The coefficient of variation or relative standard deviation (RSD) was used as a mixing indicator. It is better to examine this from an angle because no significant or general trend has been observed. The results indicate a wide variation in different classes of geometries. It was discovered that distributive mixing is more complex and highly sensitive to local flow variations [4, 18]. In the modified aspect ratio mixer, the RSD value decreases with increasing LPD angle; hence higher mixing efficiency is achieved in 120° than 90°. The case of the curved edge and standard mixers require special attention as both show extrema. In curved edge, all the angles show the best mixing efficiency than every other geometry except 100°. The 100° –value shows a sudden surge in RSD value, indicating poor performance. Similarly, in standard cases, the 90° and 110° show poor performance, with 110° showing the worst mixing, though the differences in RSD values of 90°, 100°, 110°, and 120° are not significant.

In DPM, the solver tracks the particles while advancing the flow field, and the RSD value is calculated using samples taken at the outlet of the mixers. If the solver fails to track some particles, the RSD value is affected. This number of particles that are trapped in the mixer is usually presented as transmission probability. Due to recirculation and dead zones, some particles are trapped, resulting in low transmission and higher RSD values. It explains the high RSD values of standard 90°, 110°, and curved Edge 100°. It is thus concluded that DPM is more suited for aggressive geometries at low Re numbers. Also, the presence of dead zones can be an important indicator of low mixing efficiencies. Amongst all, the curved edge gives the best distributive mixing, and more specifically, the curved edge 120° gives the lowest RSD value [10, 14].

It observing the behavior of the mixer, it is concluded that most of the pressure was dropping due to the presence of the elliptical part, which can be seen in Fig. 11 (f), showing the pressure profile through the length of the mixer. Hence, some alterations must be done to minimize the dropping pressure effect of the elliptical part. The optimization

can be done by serrations as well, which can improve the performance of the mixer. Also, in the case of Curved Edge Kenics, when blended the edges of Kenics were employed, a better trend is observed than the standard one. Hence, it is recommended to conduct a study on the serrated elliptical part either of triangular, circular or squared serration, as done with SMX mixer, which can strengthen the mixing efficiency and minimizes the pressure drop through the mixer [5, 7, 17, 20].

Eulerian Multiphase VOF model is recommended for observing mixing behavior and evaluation of mixing efficiency in static mixtures, as it is designed for both continuous-continuous phase interactions and dispersed-continuous phase interaction. The continuity equation is solved for each phase, so it is very computationally expensive but gives accurate liquid-liquid or solid-liquid mixing. Eulerian multi-phase model limits the number of secondary phases because as it is very memory intensive, so it requires greater memory to model the number of secondary phases. By observing the performance of modified Kenics with increased length, it can be predicted that if the length of Kenics decreases, the contact surface for fluid would be minimized, resulting in an improvement in pressure drop. Also, the twist angle in shorter length causes aggressive fluid mixing compared to standard and long Kenics. Heat transfer will also enhance if better mixing is achieved. So, a short aspect ratio is recommended but for low Re numbers. The pressure drop of the static mixer is significantly reduced just by blending the edges of Kenics. A study was conducted in which the effect of different blend radius on the z factor was observed, and it shows the inverse relation between blend radius and z factor. Further investigation of blend edges is recommended with a different combination of elements as it shows significant improvement in pressure drop at high Reynold numbers.

CONCLUSIONS

In the light of these results, it is concluded that in the analyzed flow regime, Curved Edge Kenics is the most promising. They give the moderate pressure drop, high dispersive mixing resulting in high heat transfer of distributive mixing in DPM. Amongst the different angles of Curved Edge, 120° is the best option. These results and the superiority of Curved Edge Kenics can be extended to low Reynold numbers as well, as it will result in further

improvement of Curved Edge over other mixers. The study on blend radii reveals another trend of Curved Edge Kenics for low Reynold numbers. It supersedes the performance of standard TEET mixer in heat transfer analysis for Reynold number less than 100 Curved Edge Kenics shows better heat transfer capabilities than standard cases. Hence, it is recommended to study the heat transfer performance of Curved Edge Kenics and Standard TEET mixer observing at low Reynold numbers to assess the extent of improvement. The modification can be made in the field of perforation and serration. The mixing performance and pressure drop factor can be optimized using perforations and serrations. The number of perforations can be made in mixing geometries, the twisted element, and the elliptical element, which may enhance the mixer's performance by decreasing the pressure drop with improved mixing performance of the static mixer. Also, the performance can be improved by using the perforation of different diameters in size in the mixing elements.

Nomencluture

Length	L, cm
Diameter	d, cm
Twist angle	α, degree
Crossing angle	β, degree
Slope angle	β / 2, degree
Spacing	x, cm

Abbreviations

LPD	Low-Pressure Drop
CFD	Computational Fluid Dynamics
SM	Static Mixer
SMX	Static Mixer Type X
SMV	Static Mixer Type V
SMQ	Static Mixer Quatro Shaped
KMs	Kenics Mixers
LLPD	Low Low Pressure Drop
FDM	Finite Difference Method
FEM	Finite Element Method
FVM	Finite Volume Method
DPM	Discrete Phase Model
Re	Reynold's number
HTC	Heat Transfer Coefficient
STD	Standard Deviation
RSD	Relative Standard Deviation
ISG	Interfacial Surface Generator

Acknowledgment

REFERENCES

[1] Bunkluarb N., Sawangtong W., Khajohnsaksumeth N., Wiwatanapataphee B., Numerical Simulation of Granular Mixing in Static Mixers with Different Geometries, *Adv. Diff. Equ.*, **2019**: 1-17 (2019).

[2] Ouda M., Al-Ketan O., Sreedhar N., Hasan Ali M.I., Abu Al-Rub R.K., Hong S., Arafat H.A., Novel Static Mixers Based on Triply Periodic Minimal Surface (TPMS) Architectures, *J. Environ. Chem. Eng.*, **8**: 1-11 (2020).

[3] Soman S.S., Madhuranthakam C.M.R., Effects of Internal Geometry Modifications on the Dispersive and Distributive Mixing in Static Mixers, *Chem. Eng. Process.*, **122**: 31-43 (2017).

[4] Jegatheeswaran S., Ein-Mozaffari F., Wu J., Process Intensification in a Chaotic SMX Static Mixer to Achieve an Energy-Efficient Mixing Operation of Non-Newtonian Fluids, *Chem. Eng. Process.*, **124**: 1-10 (2018).

[5] Göbel F., Golshan S., Norouzi H.R., Zarghami R., Mostoufi N., Simulation of Granular Mixing in a Static Mixer by the Discrete Element Method, *Powder Technol.*, **346**: 171-179 (2019).

[6] Jung S.Y., Ahn K.H., Kang T.G., Park G.T., Kim S.U., Chaotic Mixing in a Barrier-Embedded Partitioned Pipe Mixer, *AIChE J.*, **64**: 717-729 (2018).

[7] Stec M., Synowiec P.M., Study of Fluid Dynamic Conditions in the Selected Static Mixers Part III—Research of Mixture Homogeneity, *Can. J. Chem. Eng.*, **97**: 995-1007 (2018).

[8] Gurieff N., Keogh D.F., Timchenko V., Menictas C., Enhanced Reactant Distribution in Redox Flow Cells, *Molecules*, **24**: 1-10 (2019).

[9] Saad M.A.M., Elamari A.A., Alshebani A.E., Elmabrouk E.M., Abukanisha S.I., Static Mixers for Water Ozonation: Applications and Mathematical Modelling - A Review, *J. Pure Appl. Sci.*, **19**: 59-72 (2020).

[10] Meng H.-B., Song M.-Y., Yu Y.-F., Jiang X.-H., Wang Z.-Y., Wu J.-H., Enhancement of Laminar Flow and Mixing Performance in a Lightnin Static Mixer, *Int. J. Chem. React. Eng.*, **15**: 1-21 (2017).

[11] Gidde R.R., Shinde A.B., Pawar P.M., Ronge B.P., Design Optimization of a Rectangular Wave Micromixer (RWM) Using Taguchi Based Grey Relational Analysis (GRA), *Microsyst. Technol.*, **24**: 3651-3666 (2018).

[12] Vasilev M.P., Abiev R.S., Intensity and Efficiency of Droplet Dispersion: Pulsating Flow Type Apparatus vs. Static Mixers, *Chem. Eng. Res. Des.*, **137**: 329-349 (2018).

[13] Alekseev K.A., Mukhametzyanova A.G., Classification, Function, and Construction of Modern Static Mixers, *Chem. Pet. Eng.*, **55**: 934-942 (2020).

[14] Xu C., Zhong Y., Zheng Y., Huang W., Jin C., Xu B., Yao R., Feng Z., Micromixing-Assisted Preparation of TiO2 Films from Ammonium Hexafluorotitanate And Urea by Liquid Phase Deposition Based on Simulation of Mixing Process in T-Shaped Micromixer, *Ceram. Int.*, **45**: 11325-11334 (2019).

[15] Castro A., Helver N.L., Granada G.S., Gonzalez J., Nunhez, Assessment of the Use of Static Mixers for the Dilution of Heavy Oils with The Use of a Computational Fluid Dynamics Model, *Braz. J. Chem. Eng.*, **38**: 1-19 (2020).

[16] Mukhametzyanova A.G., Alekseev K.A., Galimov F.F., Numerical Simulation of Flow Hydrodynamics in Irregular Packing Layer, *Chem. Pet. Eng.*, **52**: 90-95 (2016).

[17] Kjær L.S., Poulsen M., Sørensen K., Condra T., Modelling of Hot Air Chamber Designs of a Continuous Flow Grain Dryer, *Eng. Sci. Tech. Int. J.*, **21**: 1047-1055 (2018).

[18] Vasilev M.P., Abiev R.S., Turbulent droplets Dispersion in a Pulsating Flow Type Apparatus – New Type of Static Disperser, *Chem. Eng. J.*, **349**: 646-661 (2018).

[19] Iqbal S., Bibi I., Ata S., Kamal S., Ibrahim S.M., Iqbal M., Gd and Co-Substituted LaNiO$_3$ and their Nanocomposites with r-GO for Photocatalytic Applications, *Diamond Relat. Mater.*, **110**: 1-14 (2020).

[20] Dharavath M., Manna P., Sinha P.K., Chakraborty D., Numerical Analysis of a Kerosene-Fueled Scramjet Combustor, *J. Therm. Sci. Eng. Appl.*, **8**: 1-7 (2016).

[21] Nemati O., Ibarra L.M.C., Fung A.S., Review of Computer Models of Air-Based, Curtainwall-Integrated PV/T Collectors, *Renewable Sustainable Energy Rev.*, **63**: 102-117 (2016).

[22] Mahmoodi H., Razzaghi K., Shahraki F., Improving Mixing Performance by Curved-Blade Static Mixer, *AIChE J.*, **66**: 1-13 (2020).

[23] Habchi C., Ghanem A., Lemenand T., Della Valle D., Peerhossaini H., Mixing Performance in Split-And-Recombine Milli-Static Mixers—A numerical Analysis, *Chem. Eng. Res. Des.*, **142**: 298-306 (2019).

[24] Mansour M., Zähringer K., Nigam K.D.P., Thévenin D., Janiga G., Multi-Objective Optimization of Liquid-Liquid Mixing in Helical Pipes Using Genetic Algorithms Coupled with Computational Fluid Dynamics, *Chem. Eng. J.*, **391**: 1-13 (2020).

[25] Belhout C., Bouzit M., Menacer B., Kamla Y., Ameur H., Numerical Study of Viscous Fluid Flows in a Kenics Static Mixer, *Mechanics*, **26**: 206-211 (2020).

[26] Haddadi M.M., Hosseini S.H., Rashtchian D., Olazar M., Comparative Analysis of Different Static Mixers Performance by CFD Technique: An Innovative Mixer, *Chin. J. Chem. Eng.*, **28**: 672-684 (2020).

[27] Hussain Z., Zaman M., Nadeem M., Ullah A., CFD Modeling of the Feed Distribution System of a Gas-Solid Reactor, *Iran. J. Chem. Chem. Eng. (IJCCE)*, **38**: 233-242 (2019).

[28] Hassan M., Razzaghi K., Shahraki F., Improving Mixing Performance by Curved-Blade Static Mixer, *AIChE J.*, **66**: 1-13 (2020).